Arnold Mathematical Journal
Volume 12, Issue 1, 2026

Foam cobordism and the Sah-Arnoux-Fathi invariant

Mee Seong Im Mikhail Khovanov

Received 18 Oct 2024; Accepted 22 Jun 2025

Abstract: This is the first in a series of papers where scissor congruence and K-theoretical invariants are related to cobordism groups of foams in various dimensions. A model example is provided where the cobordism group of weighted 1-foams is identified, via the Sah–Arnoux–Fathi invariant, with the first homology of the group of interval exchange automorphisms and with the Zakharevich first K-group of the corresponding assembler. Several variations on this cobordism group are computed as well.

AMS Classification: 37E05, 37E99, 18M30, 19D99

Key words and phrases: Foams, foam cobordism, Sah-Arnoux-Fathi invariant, interval exchange transformations, train tracks

DOI: 10.56994/ARMJ.012.001.001

1 Introduction

In link homology by a *foam*, one usually means a 2-dimensional finite combinatorial CW-complex F, often embedded in $\mathbb{R}^3$, where each point has one of the three types of neighborhoods shown in Figure 1 below. Foams are used in algebraically-defined link homology to build state spaces of planar graphs, which are then combined into complexes that define the homology of a link [16, 20, 30, 28, 17]. Foams also appear in Kronheimer–Mrowka instanton Floer homology for 3-orbifolds [18].

Locally, the foam structure is that of a two-dimensional spine of a 3-manifold. Often, foams come with extra decorations, such as orientations, weights and other labels on facets.

In this paper, a *closed* 2*-foam* means a foam as above, with additional decorations specified. More generally, one can define a 2*-foam with boundary*, the boundary being a 1-foam. A 1*-foam* is a finite graph, possibly with loops and circle edges without vertices, and additional decorations. Splitting the boundary of a 2-foam F into two disjoint sets of components, $\partial F = (-U_0) \sqcup U_1$, allows one to view F as a cobordism between 1-foams U_0 and U_1. Decorations of U_0, U_1 are induced from those of F.

This paper is the first in a series of papers which aim to use foams, in all dimensions n and with additional decorations, to understand K-theoretical structures. One expects that n-dimensional foams decorated by objects and morphisms of an exact category $\mathcal{C}$, modulo concordances which are $\mathcal{C}$-decorated $(n+1)$-dimensional foams, carry information about the n-th K-theory group $K_n(\mathcal{C})$ of $\mathcal{C}$. Facets, respectively, seams of a foam are decorated by flat connections with objects of $\mathcal{C}$, respectively short exact sequences of $\mathcal{C}$, as fibers of these flat bundles. This relation between decorated foams and algebraic K-theory is started to be studied in [9].

The present paper works out a straightforward example of this correspondence, where the abelian group of suitably decorated one-dimensional foams modulo 2-dimensional cobordisms is identified with the group $\mathbb{R} \wedge_{\mathbb{Q}} \mathbb{R}$, which is the first homology of the group of

interval exchange transformations [36]. The related invariant of interval exchange transformations mapping a group element to its image in the first homology is known as the Sah–Arnoux–Fathi invariant, or SAF invariant, for short [34, 8]. I. Zakharevich interpreted the SAF invariant map via the K_1 group of a suitable *assembler* category [37, 38], and that category plays the role of the exact category $\mathcal{C}$ above. In the present paper, we relate these structures to two-dimensional cobordisms between decorated one-dimensional foams.

In Section 2, we work out this new interpretation of the SAF invariant, as classifying elements of the cobordism group of *weighted* oriented 1-foams. In this construction, edges of an oriented 1-foam are decorated by positive real numbers a, with compatibility relations on these numbers at the vertices. The cobordism group of such foams is identified with the abelianization of the group of interval exchange transformations (IETs) in Theorem 2.6. The isomorphism uses the Sah–Arnoux–Fathi invariant of IETs, extended to arbitrary weighted oriented 1-foams.

Section 3 considers the cobordism group of planar unoriented weighted 1-foams and identifies it with the abelian group generated by brackets $[a, b]$ with $a, b \in \mathbb{R}_{>0}$ modulo the antisymmetry and the 2-cocycle relations (14)-(16). It also looks at a variation on weighted embedded foams, where each facet may carry either a positive or a negative weight. Several other variations on the group of foam cobordisms are studied in Section 4. Constructions of Sections 2 and 3 can perhaps be viewed as first steps exploring the relation between foam cobordisms and dynamical systems.

2 Foams and interval exchange transformations

In this section we interpret the Sah–Arnoux–Fathi invariant of interval exchange transformations [34, 36, 8] via cobordism classes of oriented 1-foams with facets decorated by positive real numbers (called *weighted* or $\mathbb{R}_{>0}$-*decorated* 1-foams).

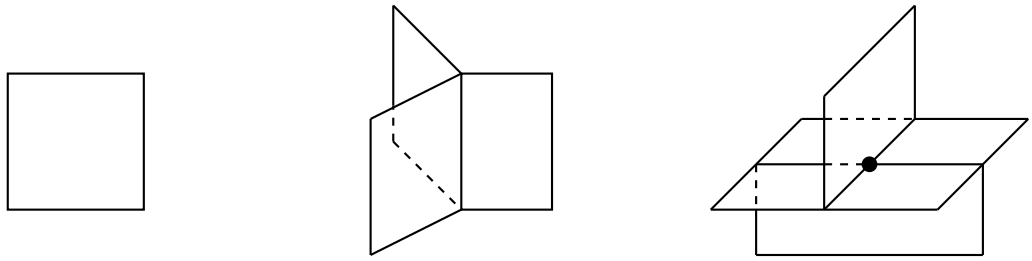

Figure 1: Three types of points on a 2-foam. Left to right: a regular point, seam points on a seam interval, a vertex.

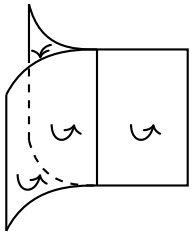

Figure 2: A choice of facet orientations and an order of thin facets near a seam of an oriented 2-foam. Facet orientations are indicated by the three "cap" semicircular arrows. The two thin facets are shown as tangent to each other along the seam, which is a convenient convention for tracking thin facets.

2.1 Oriented 1-foams and 2-foams and cobordisms between 1-foams

In this paper, a *closed 2-foam* denotes a finite combinatorial CW-complex F, where each point is one of the three types and has a neighborhood as depicted in Figure 1; these points are called *regular points*, *seam points* and *vertices* of the 2-foam, respectively. The union of seams and vertices of F is a four-valent graph $s(F)$, possibly with loops and verticeless circles. The connected components of $F \setminus s(F)$ are called the *facets* of F, and the set $s(F)$ is called the *singular points* of F.

A closed 2-foam is *oriented* if

- Each facet is oriented so that along its seams and near its vertices, the orientations match as shown in Figure 2 (for seams) and Figure 3 on the right (for vertices).

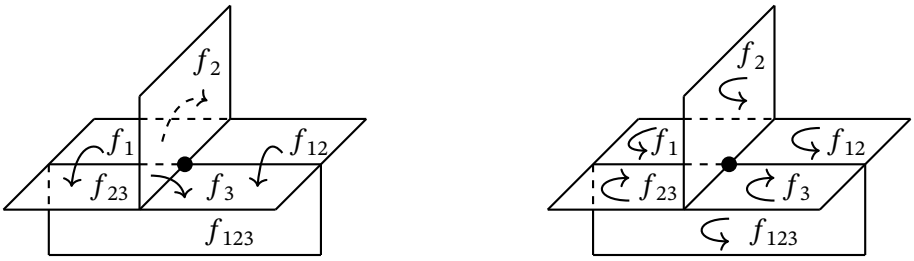

Figure 3: Left: ordering of seams near a vertex, with facets labelled f_1, f_2, f_3, f_{12}, f_{23}, f_{123}. The orderings are from smaller to larger indices: (f_1, f_2), (f_2, f_3), (f_1, f_{23}), (f_{12}, f_3). Right: one out of two possible facet orientations near a vertex is shown. Orientations and orderings must be compatible along each seam, as explained earlier and in Figure 2.

Along each seam, two of the facets are designated as *thin* and the remaining one as *thick*. The orientation of each thin facet matches (flows into) the orientation of the thick facet. Furthermore, the orientations of the two thin facets along a seam are opposite. A facet which is thin at one of its seams may be thick at another seam; this is a crucial difference from the foams mentioned at the beginning of Section 1.

- An order of two thin facets along each seam is fixed (shown by the small curly arrow from one thin facet to the other in Figure 2).

- At each vertex of the foam, the decorations (orientations and orders) of the six adjoint facets along the four seams match as follows (and shown in Figure 3 on the right). The six facets are labeled $f_1, f_2, f_3, f_{12}, f_{13}, f_{123}$. Among the triples of facets $(f_1, f_2, f_{12}), (f_2, f_3, f_{23}), (f_{12}, f_3, f_{123}), (f_1, f_{23}, f_{123})$, one triple for each seam, the first two facets are thin and the last one is thick. The facets are oriented either as shown in Figure 3 on the right or with all orientations opposite (which follows from the orientation requirements along the seams). The orders of the facets along the seams are as shown in Figure 3 on the left, in the direction of increasing indices, or the opposite (decreasing indices).

Figure 4 shows a set of three “parallel cross-sections” of a foam near a vertex, with

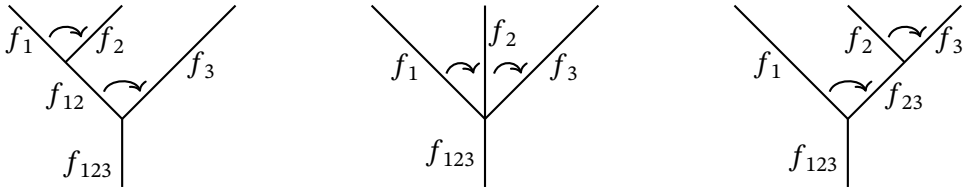

Figure 4: Three parallel cross-sections near a vertex of a 2-foam, with the middle cross-section going through the vertex. Small arrows show the order of facets along the seams.

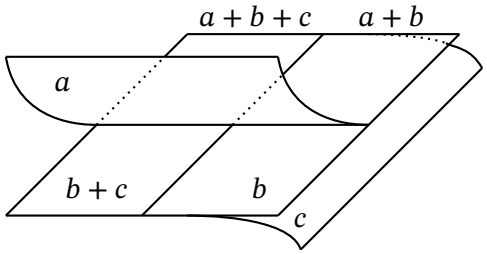

Figure 5: A vertex of a (weighted) 2-foam is analogous to that of a branched surface, c.f. [24, Figure 1.1].

one of the cross-sections going through the vertex. Figure 5 depicts a neighborhood of a vertex taking "tangencies" of the thin facets along the four seams near the vertex into account, analogous to that of a vertex in a branched surface [24, Figure 1.1], see also [27]. (For now, ignore the weights of the facets in Figure 5.)

The 1-foams can be thought of as generic cross-sections of 2-foams. A 1-foam is a finite oriented trivalent graph. At each vertex, there are two *in* edges and one *out* edge or vice versa. We call these *merge* and *split* vertices, correspondingly. They are shown in Figure 6 on the left (ignoring the weights $a, b, a+b$ in that figure). An oriented circle with no vertices on it is allowed as a component of a 1-foam. Loops are *a priori* allowed, although we will not encounter them in the present section due to working with oriented foams (they do appear in Section 3, upon consideration of unoriented foams).

It is convenient to visualize the thin edges at a merge vertex as sharing a tangent line at a vertex and think of a neighborhood of a merge vertex as a generic cross-section

across the seam of the Figure 2 foam. Likewise, a neighborhood of a split vertex of a 1-foam can be visualized as a horizontal cross-section of the rightmost foam in Figure 6. Similar conventions are used in [29, 27].

We define an oriented 2-foam F with boundary as a cobordism between oriented 1-foams U_0, U_1, where we read the morphism from bottom to top. The boundary of F is split into two disjoint 1-foams,

$$\partial F \cong (-\partial_0 F) \sqcup \partial_1 F \cong U_1 \sqcup (-U_0).$$

Away from the boundary F has a local structure that of an oriented 2-foam and collar neighborhoods near U_i, $i = 0, 1$, where it is homeomorphic to the product $U_i \times [0, \epsilon)$, $\epsilon > 0$. The orientations of the facets of F and local orders of the thin facets along the seams of F restrict to orientations of edges of its boundary 1-foams and local orders of the thin edges at the vertices of the boundary 1-foams using the standard convention for an induced orientation of the boundary of a manifold.

For completeness, we mention that an *oriented* 0*-foam* is a finite collection of points with orientations (signs + and −). It is clear how to define oriented 1-foams with boundary.

2.2 Weighted or $\mathbb{R}_{>0}$-decorated foams

Consider oriented 1-foams and 2-foams with edges (for 1-foams) and facets (for 2-foams) decorated by real numbers a for various $a > 0$ and refer to a as the *thickness*, *width*, or *label* of the facet. At a vertex of a 1-foam and a seam of a 2-foam, widths must add as shown in Figure 6. Informally, one can "thicken" the foams and think of intervals $[0, a)$ and $[0, b)$ merging into the interval $[0, a + b) = [0, a) \sqcup [a, a + b)$ at a vertex of a 1-foam and a seam of a 2-foam. This thickening is independent of a facet being thin or thick. The order of thin edges near a vertex (for 1-foams) and order of thin 2-facets near a seam (for 2-foams) matches the order of the intervals in the merge, see Figure 6.

At a vertex of a decorated 2-foam, three thin facets of thickness a_1, a_2, a_3 merge into facets of thickness $a_1 + a_2$ and $a_2 + a_3$, which then merge with the remaining thin facet

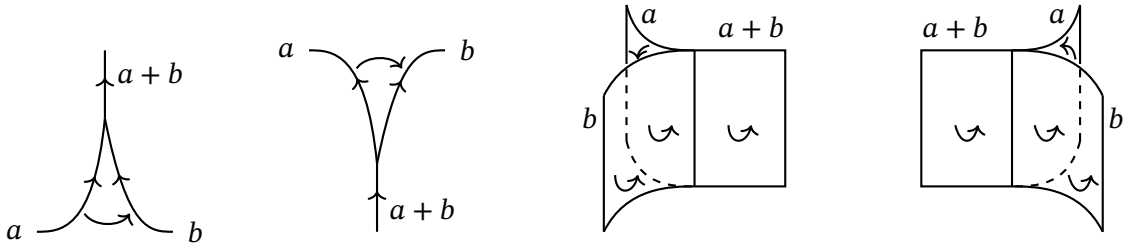

Figure 6: Left: Neighborhoods of a merge and split vertices of a weighted 1-foam, respectively. Right: neighborhoods of a point near a seam of a weighted 2-foam.

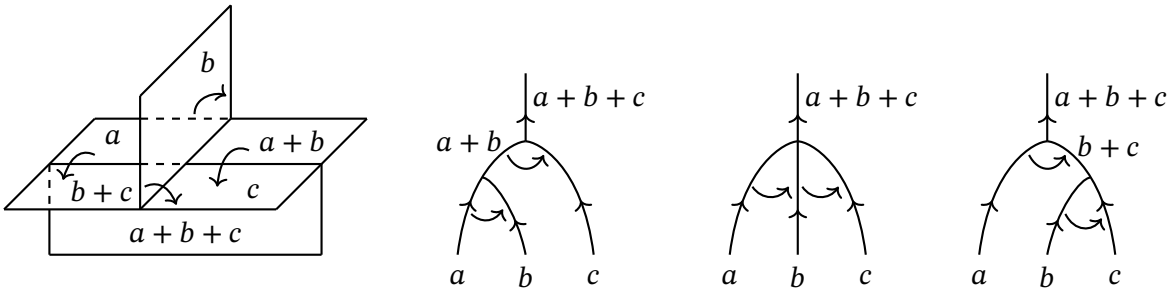

Figure 7: Left: labels near a vertex. Small arrows indicate one of the two possible orders of thin edges at each of the four seams near a vertex (orientations of facets are not shown). Right: three parellel cross-sections of this foam, including one which contains the vertex.

into the facet of thickness $a_1 + a_2 + a_3$, see Figure 7, which also shows three parallel cross-sections of this foam.

Remark 2.1. If desired, one may allow lines and facets to carry the empty interval $[0, 0)$, but this does not seem essential. Such lines and facets can then be deleted from a foam. Namely, remove all 0-weight facets. If a seam had thin facets of weights 0 and $a > 0$ along it, the seam can be hidden and thin and thick facets of thickness a along it merged into a single facet. A seam with thin facets of weights $(0, 0)$ is deleted. This operation is suitably extended to vertices with thin facets of thickness (a, b, c) at it, see Figure 7, depending on which of these three numbers are 0.

We call such foams *weighted foams* or $\mathbb{R}_{>0}$*-decorated foams* or IET*-foams* (see Sec-

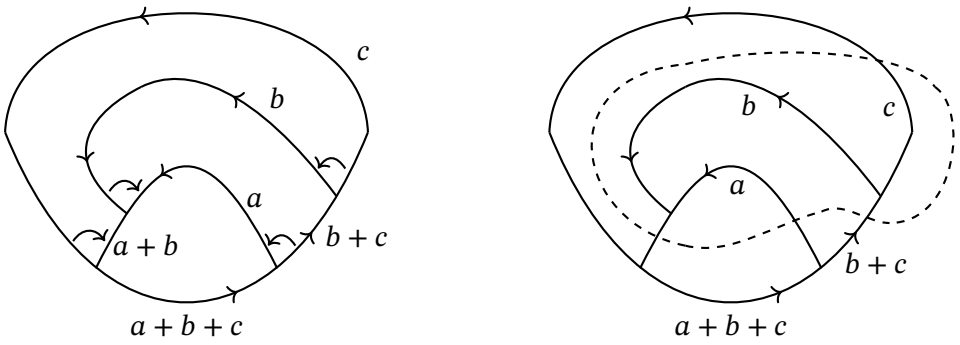

Figure 8: Left: the link of a vertex of a foam, with one possible choice of compatible orientations of facets inducing orientations of edges of the link. Likewise, one out of two possible compatible orders of thin facets at seams is shown. Right: the dashed line cuts the diagram into two pieces that appear as the two boundaries of a vertex cobordism in Figure 16, second row on the right (one of those two diagrams requires orientation reversal vs the diagram above, due to splitting the boundary into top and bottom components).

tion 2.3). The definition is straightforward to extend to all dimensions. A weighted 0-foam is a finite set of points with signs $\{+,-\}$ and weights $a>0$.

Figure 8 shows the link of a vertex of a weighted 2-foam. Weighted 2-foams are analogous to measured branched surfaces and measured laminations [23, 24], but without an embedding into a 3-manifold.

For $n=0,1$ denote by $\mathsf{Cob}^n_{>0}$ the cobordism group of weighted oriented n-foams. An n-foam U defines the trivial element $[U]=0\in\mathsf{Cob}^n_{>0}$ if and only if it bounds a weighted oriented $(n+1)$-foam.

Proposition 2.2. The cobordism group of weighted oriented 0-foams is isomorphic to $\mathbb{R}$:

$$\mathsf{Cob}^0_{>0}\ \cong\mathbb{R}. \tag{1}$$

Proof. A weighted oriented 0-foam is given by a finite collection of points decorated by signs and real weights $a>0$. Merge all $+$-decorated points into one point (adding the

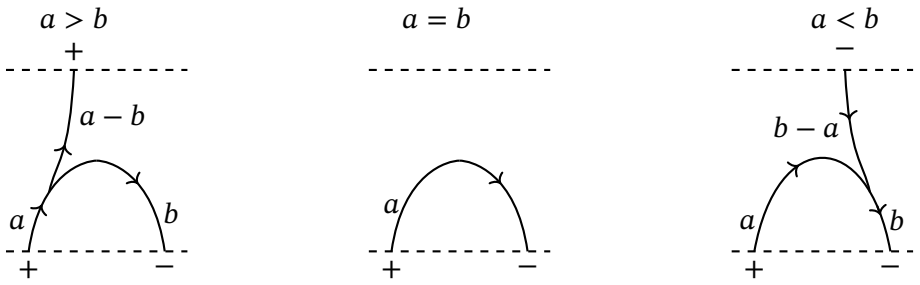

Figure 9: Merging points $(+,a)$ and $(-,b)$ via a cobordism, where $a,b>0$.

weights) and all $-$-decorated points into a point (adding the weights). The result is at most two points $(+,a),(-,b)$, which are cobordant to $(+,a-b)$ if $a>b$, $(-,b-a)$ if $a<b$, and to the empty 0-foam if $a=b$, see Figure 9.

Under the isomorphism in (1) point $(+,a)$, $a\in\mathbb{R}_{>0}$ is sent to $a\in\mathbb{R}$, point $(-,a)$ is sent to $-a\in\mathbb{R}$, and the disjoint union of signed decorated points is converted to the sum of corresponding numbers. □

2.3 Interval exchange transformations and $\mathbb{R}_{>0}$-decorated 1-foams

Pick $r\geq 1$, a decomposition $1=\sum_{i=1}^{r}\lambda_i$, $0<\lambda_i<1, \lambda_i\in\mathbb{R}$ and a permutation $\sigma\in S_r$. Interval exchange transformation $T_{\lambda,\sigma}: [0,1)\longrightarrow[0,1)$ is a bijection of a semiclosed interval to itself given by writing it as the disjoint union of r intervals

$$[0,1)=[0,\lambda_1)\sqcup[\lambda_1,\lambda_1+\lambda_2)\sqcup\ldots\sqcup[1-\lambda_r,1)$$

and permuting the order of intervals according to σ, making the i-th interval $\sigma(i)$-th in the order.

The Sah–Arnoux–Fathi invariant of $T_{\lambda,\sigma}$ is an element of $\mathbb{R}\otimes_{\mathbb{Q}}\mathbb{R}$ given by

$$\mathsf{SAF}(T_{\lambda,\sigma}) := \sum_{i=1}^{r}\lambda_i\otimes t_i = \sum_i\left(\sum_{j:\sigma(j)<\sigma(i)}\lambda_i\otimes\lambda_j-\sum_{j<i}\lambda_i\otimes\lambda_j\right), \tag{2}$$

where $t_i=\sum_{j:\sigma(j)<\sigma(i)}\lambda_j-\sum_{j<i}\lambda_j\in\mathbb{R}$ is the displacement of the i-th interval by σ.

One can write $\mathsf{SAF}(T_{\lambda,\sigma})$ as a linear combination of elements $\lambda_i \otimes \lambda_j - \lambda_j \otimes \lambda_i$, $i, j \leq r$ and view it as an element of $\mathbb{R} \wedge_{\mathbb{Q}} \mathbb{R} = \Lambda^2_{\mathbb{Q}}(\mathbb{R})$, the quotient of $\mathbb{R} \otimes_{\mathbb{Q}} \mathbb{R}$ by the abelian subgroup spanned by $\lambda \otimes \lambda, \lambda \in \mathbb{R}$. Note that we have the decomposition $\mathbb{R} \otimes_{\mathbb{Q}} \mathbb{R} \cong \Lambda^2_{\mathbb{Q}}(\mathbb{R}) \oplus S^2_{\mathbb{Q}}(\mathbb{R})$, the sum of exterior and symmetric squares, and one is taking the projection onto the first summand. The invariant can also be written as follows:

$$\mathsf{SAF}(T_{\lambda,\sigma}) \;=\; 2 \sum_{i<j\,:\,\sigma(j)<\sigma(i)} \lambda_i \wedge \lambda_j, \tag{3}$$

where $a \wedge b$ denotes the image of $a \otimes b$ under the quotient map $q : \mathbb{R} \otimes_{\mathbb{Q}} \mathbb{R} \longrightarrow \Lambda^2_{\mathbb{Q}}\mathbb{R}$, since $q(a \otimes b - b \otimes a) = 2a \wedge b$.

The SAF invariant of $T_{\lambda,\sigma}$ can be written as the integral

$$\mathsf{SAF}(T_{\lambda,\sigma}) = \int_{[0,1)} 1 \otimes (T_{\lambda,\sigma}(x) - x)dx,$$

see [36, page 2]. This invariant vanishes precisely on the commutator subgroup.

Let $\mathsf{Aut}_{\mathsf{IET}}$ be the group of Interval Exchange Transformations of $[0,1)$, that is, the group of bijections $T_{\lambda,\sigma}$ as above, with the group operation given by the composition of maps. There is a short exact sequence of groups

$$1 \longrightarrow [\mathsf{Aut}_{\mathsf{IET}}, \mathsf{Aut}_{\mathsf{IET}}] \longrightarrow \mathsf{Aut}_{\mathsf{IET}} \xrightarrow{\mathsf{SAF}} \Lambda^2_{\mathbb{Q}}\mathbb{R} \longrightarrow 1. \tag{4}$$

Remark 2.3. I. Zakharevich [38] interpreted the Sah–Arnoux–Fathi invariant as describing K_1 of an appropriate assembler category. Combining this result with constructions of the present paper yields an example of the relation between K_1 group of an appropriate category and the group of 1-foam cobordisms, in a rather special case. In a forthcoming paper, we will discuss the relation between the K_1 group and the cobordism group of decorated 1-foams in greater generality.

Remark 2.4. To each interval exchange transformation $T_{\lambda,\sigma}$ as earlier, we assign a weighted 1-foam with boundary $F_{\lambda,\sigma}$ and a closed weighted 1-foam $\widehat{F}_{\lambda,\sigma}$, as shown in Figure 10. Start with a line of thickness 1 and split it into lines of thickness $\lambda_1, \ldots, \lambda_r$ from left to right. Then permute the points at the top end of the split via the permutation

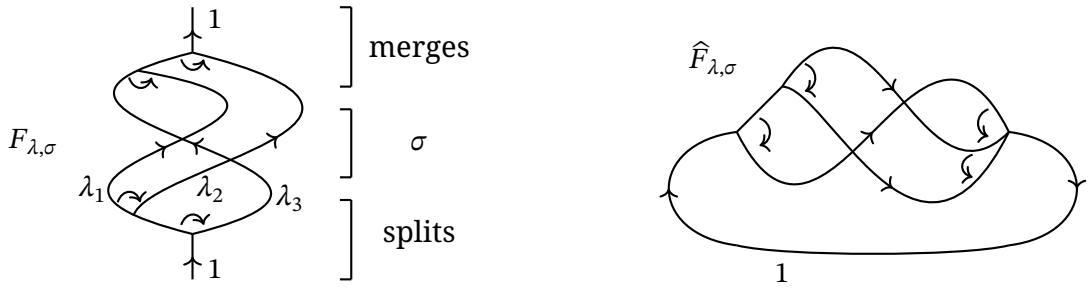

Figure 10: A foam with boundary $F_{\lambda,\sigma}$ associated to IET $T_{\lambda,\sigma}$ and its closure $\widehat{F}_{\lambda,\sigma}$. Intersections are virtual due to having to depict the foam via a projection to the plane.

$\sigma \in S_r$. After that, merge the resulting points into an interval of width 1, and close up top and bottom endpoints, both of thickness 1, into a closed diagram. Denote by $F_{\lambda,\sigma}$ the resulting weighted oriented 1-foam with boundary and by $\widehat{F}_{\lambda,\sigma}$ its closure. Intersections in Figure 10 are virtual, that is, due to having to depict the foam via a projection to the plane.

Notice that, in the cobordism group $\mathrm{Cob}^1_{>0}$, a 1-foam $\widehat{F}_{\lambda,\sigma}$ does not depend on the sequence in which the interval 1 is split into $\lambda_1, \dots, \lambda_r$ as long as in the split, $\lambda_1, \dots, \lambda_r$ go from left to right. For instance, for $r = 3$, the two sequences of splits $1 \to (\lambda_1, \lambda_2 + \lambda_3) \to (\lambda_1, \lambda_2, \lambda_3)$ and $1 \to (\lambda_1 + \lambda_2, \lambda_3) \to (\lambda_1, \lambda_2, \lambda_3)$ give rise to cobordant foams. Likewise, the sequence of merging the intervals back is irrelevant, as long as the order from left to right is $\lambda_{\sigma^{-1}(1)}, \dots, \lambda_{\sigma^{-1}(r)}$. The two 1-foams that differ in that way are then cobordant via a composition of 2-foams that create the vertices, see Figure 7. Likewise, a foam $F_{\lambda,\sigma}$, in the cobordism set of 1-foams with a fixed boundary, does not depend on the order of merges and splits.

Composition of two IETs $T_{\lambda,\sigma}$ and $T_{\lambda',\sigma'}$ is an IET $T_{\lambda'',\sigma''} = T_{\lambda',\sigma'} \circ T_{\lambda,\sigma}$ for suitable (λ'', σ'').

Proposition 2.5. The foams $\widehat{F}_{\lambda'',\sigma''}$ and $\widehat{F}_{\lambda,\sigma} \sqcup \widehat{F}_{\lambda',\sigma'}$ are cobordant. Assigning a 1-foam $\widehat{F}_{\lambda,\sigma}$

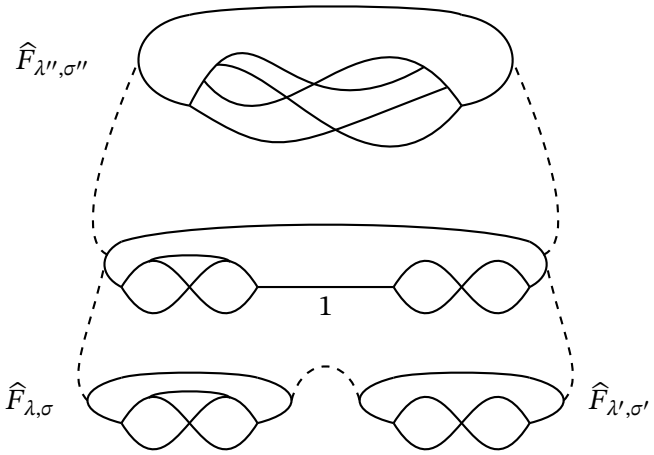

Figure 11: A schematic depiction of the cobordism from $\widehat{F}_{\lambda,\sigma} \sqcup \widehat{F}_{\lambda',\sigma'}$ to $\widehat{F}_{\lambda'',\sigma''}$ in the proof of Proposition 2.5.

to an IET $T_{\lambda,\sigma}$ extends to a homomorphism of groups

$$\phi' \ : \ \mathsf{Aut}_{\mathsf{IET}} \longrightarrow \mathsf{Cob}^1_{>0}. \tag{5}$$

Proof. The cobordism is given by first merging $\widehat{F}_{\lambda,\sigma} \sqcup \widehat{F}_{\lambda',\sigma'}$ into a connected foam, as schematically shown in the bottom half of Figure 11. The interval of thickness 1, labelled in that Figure, is then repeatedly split, by repeatedly applying elementary cobordisms shown in the second row on the right in Figure 16. These elementary cobordisms convert the 1-foam into $\widehat{F}_{\lambda'',\sigma''}$ via a foam concordance between braid-like foams, as schematically depicted in the top half of Figure 11. The rules for computing the composition $T_{\lambda',\sigma'} \circ T_{\lambda,\sigma}$ are easy to translate to a particular sequence of elementary braid-like cobordisms between these two 1-foams. □

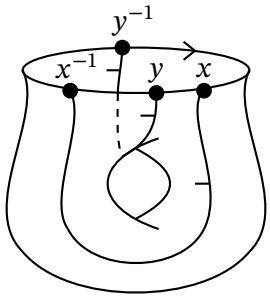

Figure 12: A commutator of IETs x, y is null-cobordant.

2.4 Cobordism group of weighted oriented 1-foams

Since the cobordism group is abelian, homomorphism ϕ' factors modulo the commutator of the automorphism group, giving a homomorphism

$$\phi \ : \ \mathrm{H}_1(\mathsf{Aut}_{\mathsf{IET}}, \mathbb{Z}) \longrightarrow \mathsf{Cob}^1_{>0}. \tag{6}$$

Figure 12 shows a cobordism from a commutator of two elements to the identity (or to the empty 1-foam).

Theorem 2.6. The homomorphism ϕ in (6) is an isomorphism of abelian groups, giving isomorphisms

$$\mathsf{Cob}^1_{>0} \ \cong \ \mathbb{R} \wedge_{\mathbb{Q}} \mathbb{R} \ \cong \ \mathrm{H}_1(\mathsf{Aut}_{\mathsf{IET}}, \mathbb{Z}) \ \cong \ K_1(\mathcal{C}_Z). \tag{7}$$

The second isomorphism is the SAF invariant, and an isomorphism $\mathrm{H}_1(\mathsf{Aut}_{\mathsf{IET}}, \mathbb{Z}) \cong K_1(\mathcal{C}_Z)$ is constructed in [38]. The category $\mathcal{C}_Z$ is the Zacharevich assembler category [38] for the IETs, also see Remark 2.7 below.

Proof. We establish an isomorphism

$$\psi \ : \ \mathsf{Cob}^1_{>0} \xrightarrow{\cong} \mathbb{R} \wedge_{\mathbb{Q}} \mathbb{R} \tag{8}$$

which is compatible with homomorphism ϕ and makes the following diagram commute

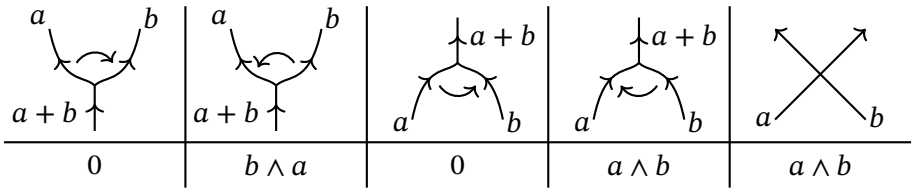

Figure 13: Contributions of splits, merges and intersections to the invariant ν.

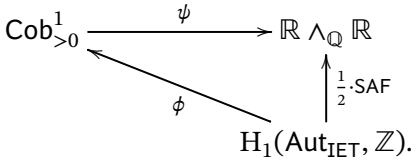

Consider a weighted oriented 1-foam U and project it generically to a plane to a diagram D.

The projection has two types of merge points and two types of split points, depending on whether the order of thin edges at a point is clockwise or counterclockwise, see Table 13.

To diagram D, assign an element $\nu(D) \in \mathbb{R} \wedge_{\mathbb{Q}} \mathbb{R}$ as a sum over local contributions:

- A split vertex with a clockwise thin edge order and a merge vertex with a counterclockwise thin edge order contribute 0. See the first split and the first merge (from left to right) in the table in Figure 13.
- For the other orientations, the contributions are shown in the table in Figure 13.
- A crossing of two intervals of lengths a and b contributes $a \wedge b$, with the orientations of the intervals determining the order of a, b in the product, see the table in Figure 13.

Some examples are shown in Figure 14. Note that ν is additive under the disjoint union of diagrams.

We claim that $\nu(D)$ depends only on the 1-foam U, that is, different plane projections result in the same invariant $\nu(D)$. Two such projections differ by local moves in Figure 15

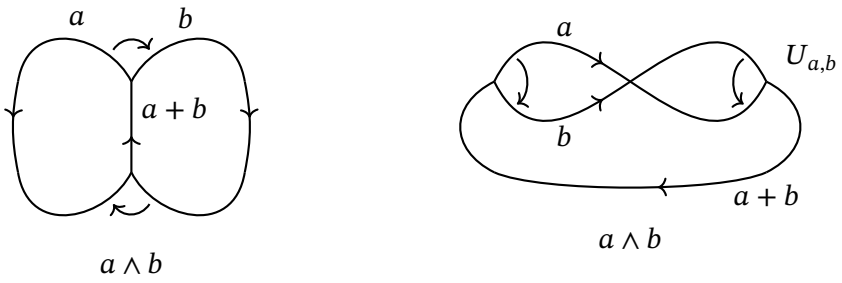

Figure 14: An invariant ν for each of these two foams is $a \wedge b$. For the foam on the left, the merge contributes $a \wedge b$ while the split contributes 0. For the foam on the right, denoted $U_{a,b}$, the intersection contributes $a \wedge b$, while both the merge and the split contribute 0. (These two foams are homeomorphic, through a homeomorphism that preserves all decorations.)

and versions of these moves given by reversing orientation of one or more of the components or reversing the order of thin edges at a vertex. This follows from the list of Reidemeister moves for embedded rigid graphs in Kauffman [14], although our case is easier, since the graphs are projected onto the plane rather than first embedded in $\mathbb{R}^3$ and then projected onto $\mathbb{R}^2$.

It is straightforward to check the invariance of ν under all variations of moves in Figure 15. For example, independent of orientations of a and b lines, invariance of ν under move 1 in Figure 15 is the relation $a \wedge b + b \wedge a = 0$. For move 2 it is $a \wedge a = 0$. Move 4 and its version for the opposite orientation determine two entries of the Figure 13 table given the other three (they determine, for instance, entries 1 and 3 of row 2 given values at entries 2, 4, 5). Move 5 corresponds to the bilinearity property of the tensor product.

Suppose that weighted 1-foams U_0, U_1 are cobordant. A cobordism between them can be realized as a finite sequence of elementary cobordisms shown in Figure 16. We can put a foam in a generic position and then take a sequence of cross-sections with minimal changes of topology between consecutive cross-sections. These changes include

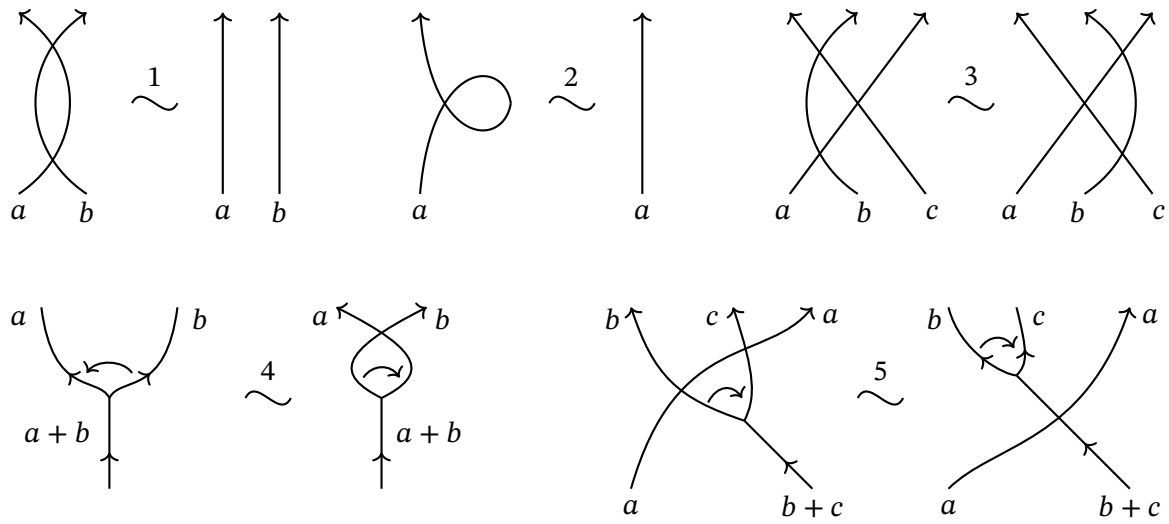

Figure 15: Diagram moves 1-5 that do not change the underlying foam.

(a) going through a vertex, which correspond to the changes in row 2 of Figure 16, (b) going through a local maximum or minimum of a seam, as shown in row 1 of Figure 16, (c) Morse critical point of a facet, as shown in row 3 on the right and the bottom row.

What remains are isotopies. The cobordism on the left of row 3 of the figure has no topology change between its top and bottom boundaries, which are different projections onto the plane of the same decorated 1-foam. This cobordism is included for completeness, and it corresponds to move 4 in Figure 15. Remaining isotopies correspond to the other moves in Figure 15.

For each elementary cobordism, one can pick diagrams for the two 1-foams at its boundaries so that they differ as shown in Figure 16. A direct computation implies that, in each case, the two diagrams have the same invariant ν.

Consequently, the homomorphism ψ in (8) is well-defined. It is clearly surjective, since each generator $a \wedge b$ is the image of some foam. Define a homomorphism

$$\psi_2 \ : \ \mathbb{R} \otimes_{\mathbb{Z}} \mathbb{R} \xrightarrow{\cong} \mathsf{Cob}^1_{>0} \tag{9}$$

by taking $a \otimes b$ to the foam in Figure 14 on the right.

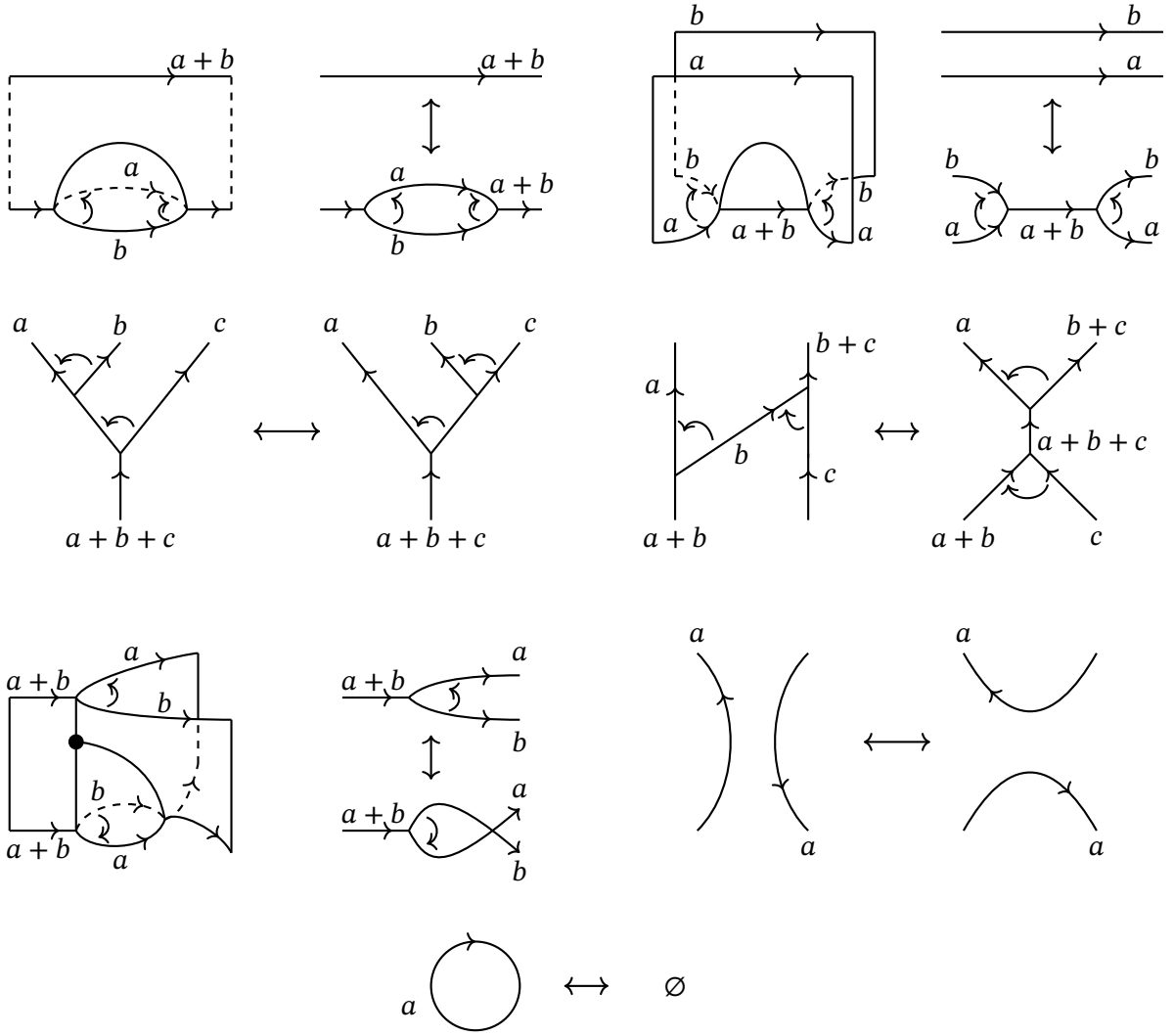

Figure 16: Top left (two pictures): a *singular cap* cobordism. Its reflection in a horizontal plane gives a *singular cup* cobordism. Top right (two pictures): a *singular saddle* cobordism. Second row: the standard cobordisms between these pairs of 1-foams are given by 2-foams with a single vertex. These transformations can also be obtained by splitting the link of a vertex into two halves, see Figure 8. Third row left (two pictures): flipping thin edges at a vertex in a diagram of a 1-foam. Third row right (two pictures): a saddle cobordism relates these two 1-foams. Bottom row: cup and cap cobordisms allow a circle to vanish or appear.

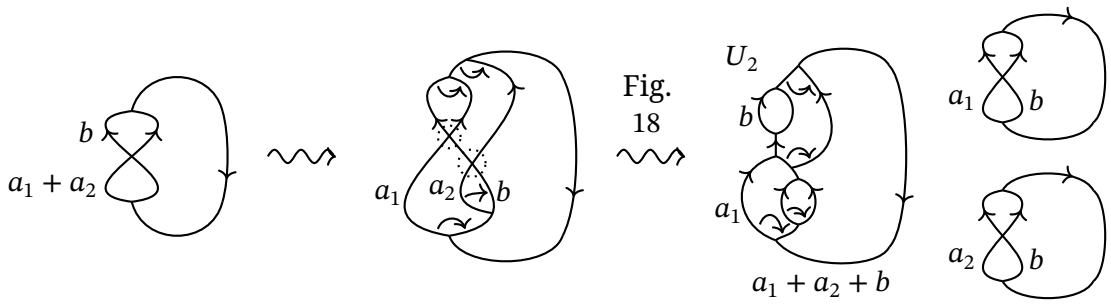

Figure 17: The cobordism for the first arrow splits the line $a_1 + a_2$ into two lines a_1 and a_2. In the second cobordism, two intersection points (with their neighborhoods indicated by dotted circles) are converted into foams $U_{a_1,b}$ and $U_{a_2,b}$, with the remaining braid-like foam U_2 cobordant to a circle of weight $a_1 + a_2 + b$; see Figure 18.

To show that ψ_2 is well-defined, we need to check the relations

$$\psi_2((a_1 + a_2) \otimes b) = \psi_2(a_1 \otimes b) + \psi_2(a_2 \otimes b), \tag{10}$$

$$\psi_2(a \otimes (b_1 + b_2)) = \psi_2(a \otimes b_1) + \psi_2(a \otimes b_2), \tag{11}$$

which also imply $n\,\psi_2(a \otimes b) = \psi_2(na \otimes b) = \psi_2(a \otimes nb)$, and, since $\mathbb{Q}$ is a divisible group, imply $\psi_2(\frac{a}{n} \otimes b) = \psi_2(a \otimes \frac{b}{n})$.

Note a related observation, that the natural quotient map $\mathbb{R} \otimes_{\mathbb{Z}} \mathbb{R} \longrightarrow \mathbb{R} \otimes_{\mathbb{Q}} \mathbb{R}$ is an isomorphism, so that (9) holds with $\mathbb{R} \otimes_{\mathbb{Q}} \mathbb{R}$ on the LHS as well.

The 1-foam $U_{a_1+a_2,b}$ associated to $(a_1 + a_2) \otimes b$ is shown in Figure 17 on the left. It is cobordant to the foam U with two crossings shown in the middle of the same figure. A crossing can be split off from any foam, as shown in Figure 18.

Splitting off both crossings from U results in the foam U_1 shown on the right of Figure 17. Foam U_1 is the union of $U_{a_1,b}, U_{a_2,b}$ and a braid-like foam U_2 with no crossings and compatible thin edge orientations at vertices. Foam U_2 is cobordant to the circle of weight $a_1 + a_2 + b$ and, then, to the empty foam. Hence, foams $U_{a_1+a_2,b}$ and $U_{a_1,b} \sqcup U_{a_2,b}$ are cobordant and the relation (10) holds. The relation (11) follows in the same way.

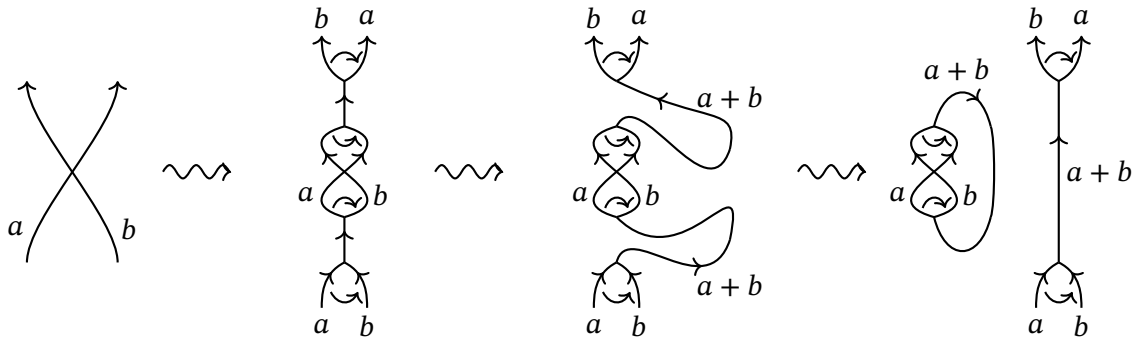

Figure 18: Converting a foam with a crossing to the union of a foam with one less crossing and foam $U_{a,b}$ shown in Figure 14 on the right.

To check that ψ_2 factors through a homomorphism

$$\psi_1 \ : \ \mathbb{R} \wedge_{\mathbb{Z}} \mathbb{R} \xrightarrow{\cong} \mathsf{Cob}^1_{>0}, \tag{12}$$

we observe that

$$\psi_2(a \otimes b + b \otimes a) = 0$$

since the disjoint union $U_{a,b} \sqcup U_{b,a}$ of 1-foams associated to $a \otimes b$ and $b \otimes a$ is null-cobordant.

To see that ψ_1 is surjective, pick a 1-foam U. This foam can be represented as the closure of a braid-like 1-foam B. Choose a diagram D of B where all splits and merges have local ν-invariant 0, see Table 13, with the closure $\widehat{D}$ describing the foam U.

All crossings can be removed from D via cobordisms shown in Figure 18. There, as a first step, parallel lines of thickness a and b above and below the crossing are merged to create two intervals, each of thickness $a + b$. They are then brought near each other and merged via a saddle point cobordism. This results in a disconnected 1-foam which is the disjoint union of foam $U_{a,b}$ and a foam with one fewer crossing versus the original.

The 1-foam $\widehat{D}$ is cobordant to the union $\widehat{D_1} \sqcup D_2$. Here $\widehat{D_1}$ is the closure of a braid-like crossingless diagram D_1 where all merges and splits have local ν-invariant 0, and D_2 is the union of foams U_{a_i,b_i}, $a_i, b_i \in \mathbb{R}_{>0}$ over all crossings (a_i, b_i) of D. The diagram D_1 is cobordant to a circle of some thickness and, hence, null-cobordant. This shows the surjectivity of ψ_1.

Composition $\psi \circ \psi_1$ is clearly identity. That and surjectivity of ψ_1 implies that $\psi_1 \circ \psi$ is the identity map. □

Remark 2.7. On the category side, we can follow Zakharevich [37, 38] and consider the category $\mathcal{C}_Z$ with objects – half-open interval $[a, b) \subset \mathbb{R}$. Morphisms are metric-preserving and order-preserving inclusions of intervals, and the *assembler* structure is given by pairs of morphisms $[a_1, b_1), [a_2, b_2) \xrightarrow{\psi_1, \psi_2} [a, b)$ that cover the interval without overlaps. More generally, given a Zacharevich assembler category $\mathcal{C}$, one can consider n-dimensional foams where facets are decorated by objects of $\mathcal{C}$, $(n-1)$-dimensional seams by coverings of $\mathcal{C}$, and so on. The cobordism group of $\mathcal{C}$-decorated n-foams should then be related to K-theory groups $K_n(\mathcal{C})$ as defined in [37]. Cobordism groups of foams decorated by objects of a category are introduced in [9].

Remark 2.8. It is possible to loosely compare the group $\mathsf{Aut}_{\mathsf{IET}}$ of IET transformations of the interval to the braid group and weighted 1-foams to links (note, though, that 1-foams are not embedded anywhere, while links are embedded in $\mathbb{R}^3$). The closure of a braid is an oriented link and the closure of an IET can be described by an oriented weighted 1-foam. The analogue of the Alexander theorem is simple: any oriented weighted 1-foam is the closure of some element of $\mathsf{Aut}_{\mathsf{IET}}$, and the analogue of the Markov theorem is straightforward to write down as well since 1-foams are not embedded in $\mathbb{R}^3$ (Markov's theorem is known in the harder case of graphs embedded in $\mathbb{R}^3$, see [12, 13, 7]). The analogue of the SAF invariant for oriented links is, perhaps, the sum of the linking numbers $\mathsf{lk}(L_i, L_j)$, $i < j$, over all pairs of components of a link L. This analogy is inspired by Figure 13, where (a, b) crossing adds $a \wedge b$ to the SAF invariant, similar to the formula for the linking number. The SAF invariant is preserved by the cobordisms of the oriented weighted 1-foams, as Theorem 2.6 shows. The linking number is invariant under some cobordisms in $\mathbb{R}^3 \times [0, 1]$ between the links in $\mathbb{R}^3$. More precisely, pick an ordered countable set S and equip a link L with a map $\psi : \mathsf{comp}(L) \longrightarrow S$ from its set $\mathsf{comp}(L)$ of connected components to S. Consider the cobordisms M between such links L, L' equipped with a map $\mathsf{comp}(M) \longrightarrow S$ which is compatible with the maps ψ, ψ' for its boundary links L, L'.

The S-linking number

$$\mathsf{lk}_S(L) \ := \sum_{i,j\,:\,\psi(i)<\psi(j)} \mathsf{lk}(L_i, L_j)$$

is invariant under such cobordisms.

Remark 2.9. In the definition of weighted foams, the abelian semigroup $(\mathbb{R}_{>0}, +)$ can be replaced by an arbitrary commutative semigroup $(H, +)$. One can then form the abelian group Cob^1_H of H-weighted oriented 1-foams modulo cobordisms. The latter are H-weighted oriented 2-foams with boundary. The above arguments extend to an isomorphism

$$H \wedge H \ \cong \ \mathsf{Cob}^1_H, \tag{13}$$

taking $a \wedge b$ to $[U_{a,b}]$. Here $H \wedge H$ is the abelian group generated by symbols $a \wedge b$, $a, b \in H$, with defining relations

$$\begin{aligned} a \wedge b + b \wedge a &= 0, \\ (a_1 + a_2) \wedge b &= a_1 \wedge b + a_2 \wedge b. \end{aligned}$$

In particular, the cobordism group of $\mathbb{R}$-decorated oriented 1-foams is isomorphic to that of $\mathbb{R}_{>0}$-decorated foams, since the natural map $\mathbb{R}_{>0} \wedge \mathbb{R}_{>0} \longrightarrow \mathbb{R} \wedge \mathbb{R}$ induced by the inclusion $\mathbb{R}_{>0} \hookrightarrow \mathbb{R}$ is an isomorphism.

There are several related ways to thicken an (oriented) $\mathbb{R}_{>0}$-weighted 1-foam to a 2-dimensional structure and a cobordism between such foams to a three-dimensional structure.

2.4.1 Lower limit topology

One can thicken an $\mathbb{R}_{>0}$-decorated 1-foam to a 2-dimensional structure by multiplying a 1-facet I carrying label a by $[0, a)$ and then gluing these products at vertices, see Figures 19, 20.

We equip intervals $[0, a)$ with the *lower limit topology* ℓ, with a basis of open sets given by $[a_1, b_1)$, with $0 \leq a_1 < b_1 \leq a$, see Munkres [22, Section 13]. With this topology, there

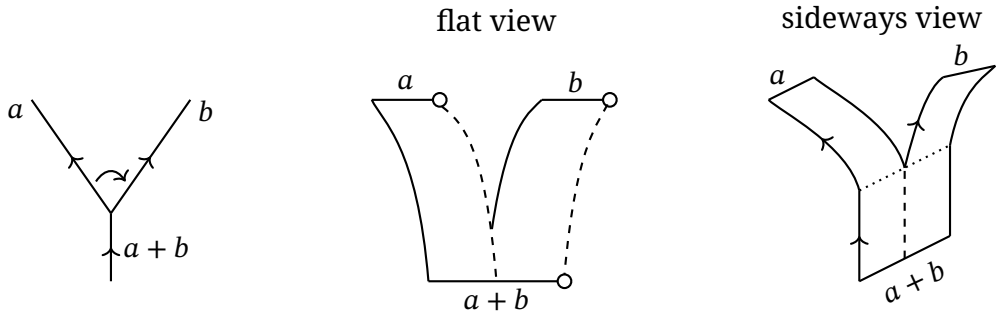

Figure 19: A split and its thickening. An IET 1-foam U can be replaced by a "surface" $T(U)$, which is locally the product $(0,1) \times [0,1)_\ell$, where ℓ denotes the lower limit topology, also see Figure 20.

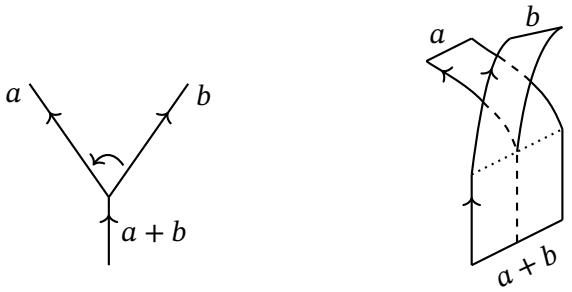

Figure 20: A split with the opposite thin edge orientation vs. the one in Figure 19 and its thickening, shown sideways.

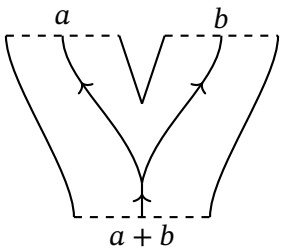

Figure 21: A weighted oriented 1-foam can be thickened to a weighted oriented train track on an oriented surface with boundary.

are homeomorphisms $[0,a) \sqcup [0,b) \cong [0,a+b)$ given by placing $[0,b)$ immediately to the right of $[0,a)$.

In this way, a 1-foam U as above is thickened to a topological space $T(U)$ which is locally homeomorphic to the product $[0,1)_\ell \times (0,1)$. A cobordism between two such 1-foams is thickened to a topological space locally homeomorphic to $[0,1)_\ell \times (0,1)^2$.

This thickening of 1-foams and 2-foams is related to the Zakharevich assembler category, see Remark 2.7 above and the discussion in the introduction.

The topological space $T(U)$ associated to a 1-foam U carries a foliation where connected components of the leaves are locally $x \times (0,1)$ for $0 \leq x < a$. If all leaves are compact (and then necessarily homeomorphic to $\mathbb{S}^1$), the foam U is null-cobordant. The opposite implication fails, since $U \sqcup U^!$ is null-cobordant for any U, where $U^!$ is the mirror image of U.

2.4.2 Train tracks on surfaces

A weighted oriented 1-foam can be thickened to an oriented train track [25] on a surface with boundary, see Figure 21. Transformations of unoriented train tracks that do not change the associated measured foliation or measured lamination [25, Sections 2.1, 2.3] can be interpreted as the cobordisms of train tracks in $S \times [0,1]$, where S is the surface that contains the train track.

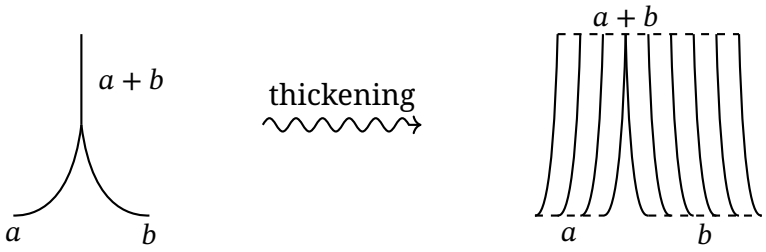

Figure 22: Thickening an embedded (a, b) vertex to a flow.

Remark 2.10. Interval exchange transformations can be thickened to very flat surfaces, or translation surfaces [39, 40], i.e., surfaces with a flat metric and singular points where total angles at these points are multiples of 2π. Oriented weighted 1-foams, equipped with additional data, can likewise be thickened to very flat surfaces (we omit the details).

3 Planar unoriented weighted foams and antisymmetric 2-brackets

Consider unoriented weighted 1-foams U embedded in the plane $\mathbb{R}^2$, and denote an embedded foam also by U. Such a foam U is analogous to a weighted unoriented train track on a surface [25], except that no conditions are imposed on the Euler characteristic of components of the complement of U in $\mathbb{R}^2$ (compare with [25, Section 1.1]). An embedded 1-foam can be thickened to an open subset of $\mathbb{R}^2$ with an unoriented bidirectional flow on it, see Figure 22.

By a cobordism between two unoriented embedded 1-foams U_0, U_1, we mean an unoriented embedded 2-foam $V \subset \mathbb{R}^2 \times [0,1]$ so that $V \cap (\mathbb{R}^2 \times \{i\}) = U_i$, $i = 0, 1$. Note that for any 1-foam U, the disjoint union $U \sqcup U^!$ of U with its mirror image is null-cobordant. See Figure 23 for an example of the mirror image of an unoriented embedded foam.

Denote by $\mathsf{Cob}^{1,\mathrm{up}}_{\mathbb{R}_{>0}}$ the set of cobordism classes of unoriented embedded 1-foams ("up" in the superscript stands for *unoriented planar*). The disjoint union and mirror image

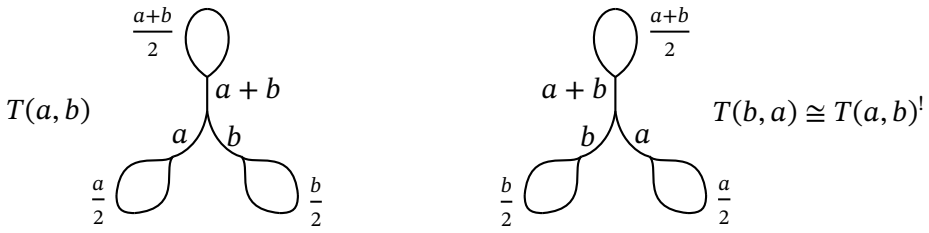

Figure 23: The tripod 1-foam $T(a,b)$ and its mirror image $T(a,b)^! \cong T(b,a)$.

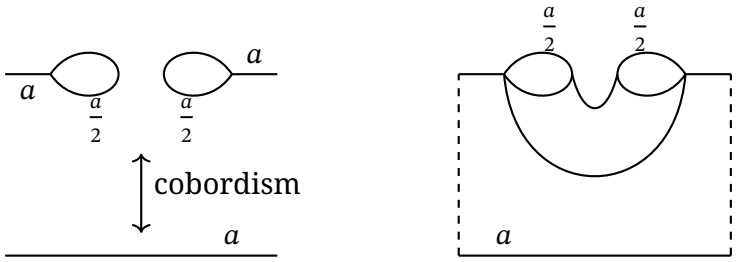

Figure 24: A cobordism between an interval and two looped half-intervals (lollipops).

operations turn this set into an abelian group. Denote by $[U]$ the image of a 1-foam U in that group.

In general, there is no obvious cobordism between U and $U^!$ (and we will see that $[U] \neq [U^!]$, in general).

For $a, b > 0$ denote by $T(a,b)$ the 1-foam shown in Figure 23, which we also call a *tripod foam*. Note that $T(a,b)^! := T(b,a)$.

Proposition 3.1. The group $\mathrm{Cob}^{1,\mathrm{up}}_{\mathbb{R}_{>0}}$ is generated by symbols $[T(a,b)]$ of tripod 1-foams over all $a, b > 0$.

Proof. The cobordism shown in Figures 24, 25 allows to convert an interval into two looped half-intervals. The loop at the end of an a-interval has thickness $a/2$. This cobordism can be applied at each edge of U, as shown in Figure 26 on the left, to cut U into a union of tripod foams and circles. Each circle can further be cut into a barbell foam (the latter is shown in Figure 27, together with a cobordism from it to the empty foam, in

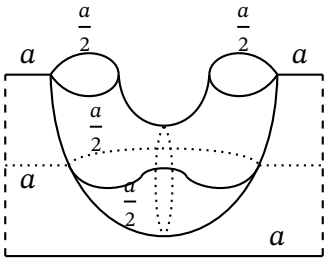

Figure 25: The cobordism from Figure 24 in more detail.

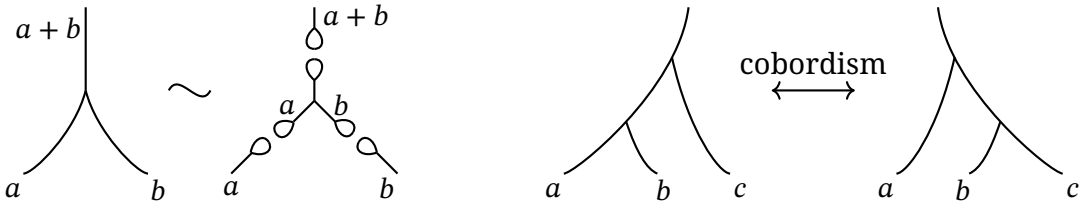

Figure 26: Left: splitting off a vertex of a planar 1-foam into the tripod $T(a,b)$, see also Figure 23 on the left. Right: existence of a cobordism between these 1-foams combined with the splittings on the left corresponds to the relation $[a,b]+[a+b,c]=[b,c]+[a,b+c]$ in $Z^2(\mathbb{R}_{>0})$, see proof of Proposition 3.3 below.

the top right corner of the figure). If a foam U has vertices $v_1,\dots,v_n$ with thin edges at the vertex v_i of thickness (a_i,b_i), going counterclockwise, then $[U]=\sum_{i=1}^{n}[T(a_i,b_i)]$. □

Remark 3.2. Figure 28 shows that $T(a,b)$ is cobordant to $T(a,b-a)$ if $a<b$. Passing to mirror images shows that $T(a,b)$ is cobordant to $T(a-b,b)$ if $a>b$. These cobordisms can be iterated to a foam cobordism version of the Euclidean division algorithm. In particular, iterating these operations we see that $T(a,b)$ is null-cobordant if $b\in\mathbb{Q}a$ (that is, if a and b are proportional over $\mathbb{Q}$). Cobordism between $T(a,a)$ and the empty foam is shown in the second row in Figure 27.

Consider 1-foams in the first two rows of Figure 16, ignoring the orientations of edges and orders of thin edges at vertices and instead viewing the 1-foams as planar (embedded

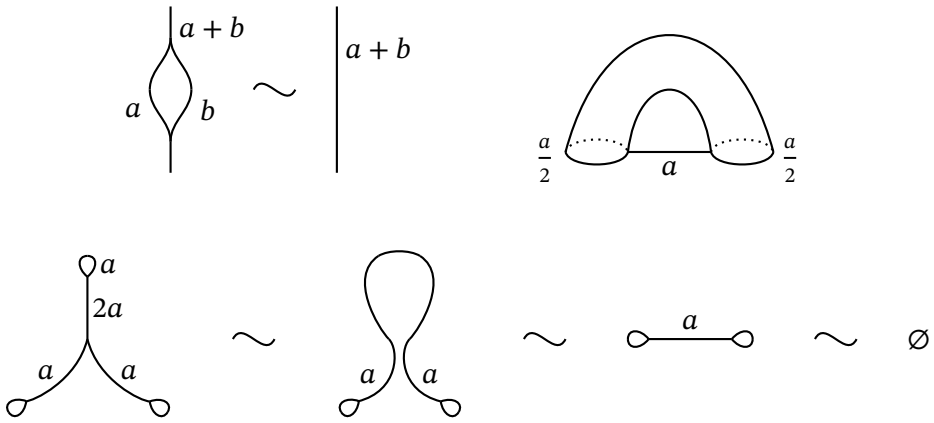

Figure 27: Top left: the two foams there are cobordant, which corresponds to the relation $[a,b]+[b,a]=0$ (see proof of Proposition 3.3 below). Top right: barbell 1-foam is null-cobordant (encoding the last cobordism in the bottom row). Bottom row: foam $T(a,a)$ is cobordant to a barbell foam and null-cobordant (relation $[a,a]=0$).

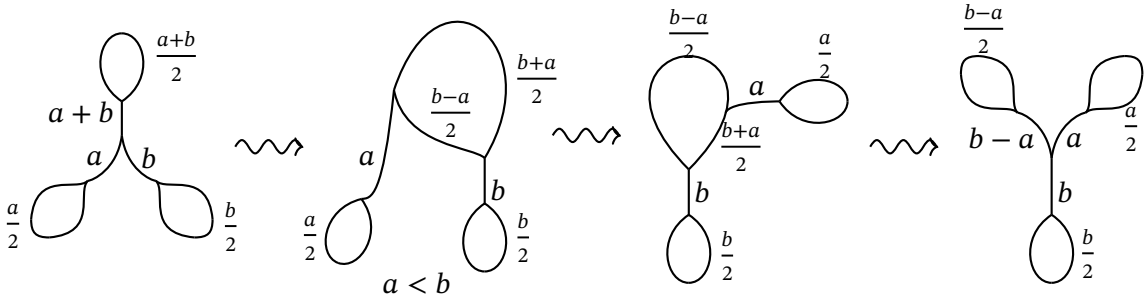

Figure 28: A cobordism between $T(a,b)$ and $T(a,b-a)$, for $a<b$.

in $\mathbb{R}^2$). These 1-foams are cobordant in pairs, via 2-foam cobordisms embedded in $\mathbb{R}^2\times[0,1]$. At the same time, breaking up these 1-foams along edges results in disjoint unions of the foam $T(x,y)$ for various $x,y\in\mathbb{R}_{>0}$. Passing to the cobordism group and replacing $\mathbb{R}_{>0}$ by a commutative semigroup H motivates the following definition.

Given a commutative semigroup $(H,+)$, denote by $Z^2(H)$ the abelian group with generators $[a,b]$, $a,b\in H$, and defining relations

$$[a,a] = 0, \quad a\in H, \tag{14}$$

$$[a,b]+[b,a] = 0, \quad a,b\in H, \tag{15}$$

$$[a,b]+[a+b,c] = [a,b+c]+[b,c], \quad a,b,c\in H. \tag{16}$$

Note that relation (14) does not imply the skew-commutativity relation (15) since the bracket $[a,b]$ is not bilinear. Equations (14) and (15) together are the strong version of the skew-commutativity property in the absence of bilinearity. Equation (16) is reminiscent of the 2-cocycle relation – the difference between the two sides can be interpreted as the signed boundary of a 3-simplex with oriented edges labeled $a,b,c,a+b,b+c,a+b+c$. This is explained in Figure 29. The analogue of symbol $[x,y]$ is an oriented triangle with oriented sides labeled $x,y,x+y$. The oriented boundary of a 3-simplex with sides labeled by a,b,c and their sums is the difference between the right-hand side and left-hand side of equation (16). Also see [11, Section 2.4].

We call $Z^2(H)$ *the antisymmetric 2-bracket* or *antisymmetric 2-cocycle of* H.

A homomorphism $f : H_1 \longrightarrow H_2$ of commutative semigroups induces a homomorphism $Z^2(H_1)\longrightarrow Z^2(H_2)$.

Proposition 3.3. The cobordism group $\mathsf{Cob}^{1,\mathsf{up}}_{\mathbb{R}_{>0}}$ of planar unoriented weighted 1-foams is isomorphic to $Z^2(\mathbb{R}_{>0})$:

$$\mathsf{Cob}^{1,\mathsf{up}}_{\mathbb{R}_{>0}} \cong Z^2(\mathbb{R}_{>0}), \tag{17}$$

taking $[T(a,b)]$ to $[a,b]$ for all $a,b>0$.

Proof. Consider the free abelian group Z on generators $[a,b]'$, over all $a,b\in\mathbb{R}_{>0}$. Proposition 3.1 says that there is a surjective homomorphism $\tau : Z\longrightarrow \mathsf{Cob}^{1,\mathsf{up}}_{\mathbb{R}_{>0}}$ taking $[a,b]'$ to

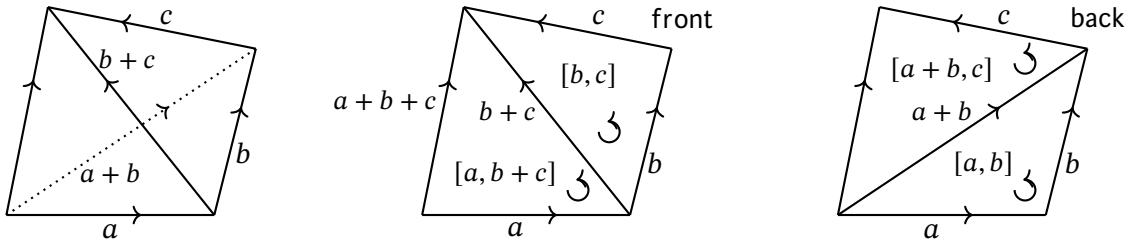

Figure 29: We have $\partial(\Delta^3) = \mathsf{front} - \mathsf{back} = [a, b+c] + [b, c] - ([a, b] + [a+b, c])$. Equation $\partial(\Delta^3) = 0$ is then the relation (16).

$[T(a, b)]$. Furthermore, relations (14)-(16) hold for the images of $[a, b]'$ under τ. Indeed, $T(a, a)$ is null-cobordant, giving the relation $\tau([a, a]') = 0$. The disjoint union $T(a, b) \sqcup T(b, a)$ is null-cobordant, implying

$$\tau([a, b]' + [b, a]') = 0. \tag{18}$$

It is convenient to pair up a- and b-lollipop ends of $T(a, b) \sqcup T(b, a)$ and pass to the 1-foam which is a split of $(a + b)$-strand into a- and b-strands, followed by the merge, see Figure 27 top left. There is a natural cobordism from the split-merge to the $(a + b)$-strand, which is another way to see the relation (18). Ignoring orientations and edge orders, this cobordism is depicted in the top left corner of Figure 16. Likewise, that

$$\tau([a, b]') + \tau([a + b, c]') = \tau([a, b + c]') + \tau([b, c]') \tag{19}$$

follows from the existence of a cobordism between the two ways to merge the parallel a, b, c-strands into $(a + b + c)$-strand, see Figure 26 on the right. For example, there is the one-vertex cobordism between these two 1-foams.

Consequently, the homomorphism τ descends to a surjective homomorphism, also denoted

$$\tau \ : \ Z^2(\mathbb{R}_{>0}) \longrightarrow \mathsf{Cob}^{1,\mathsf{up}}_{\mathbb{R}>0}. \tag{20}$$

Vice versa, breaking a planar weighted 1-foam into tripods gives a map τ' from planar foams into $\mathbb{Z}$-linear combinations of symbols $[a, b]'$, and we would like to turn τ' into the inverse of τ. A cobordism between two 1-foams can be represented as a composition of

elementary cobordisms, including vertex cobordisms, singular saddles, cups and caps, and the usual saddle, cup and cap cobordisms between 1-manifolds. These cobordisms do not change the linear combination of symbols $[a,b]$ associated to a 1-foam, when viewed as an element of $Z^2(\mathbb{R}_{>0})$.

Note that the relation $[a,a]=0$ in (14) does not come from any elementary cobordism. The tripod $T(a,a)$ is null-cobordant, however, as shown in Figure 27. This discrepancy has the following explanation. When breaking a tripod $T(a,b)$ along every edge to construct the map τ', one adds three more terms to $[a,b]'$ due to the three lollipop vertices of the tripod, so that the composition of τ and τ' is

$$[a,b]' \xrightarrow{\tau} [T(a,b)] \xrightarrow{\tau'} [a,b]' + [a/2,a/2]' + [b/2,b/2]' + [(a+b)/2,(a+b)/2]'.$$

In particular, the composition $\tau'\tau$ differs from the identity due to the presence of three terms $[x,x]'$ for $x \in \{a/2, b/2, (a+b)/2\}$. Setting these terms to 0 in $Z^2(\mathbb{R}_{>0})$ makes the composition $\tau'\tau = \mathsf{id}$, where now τ' is a well-defined map

$$\tau' \ : \ \mathsf{Cob}^{1,\mathsf{up}}_{\mathbb{R}>0} \longrightarrow Z^2(\mathbb{R}_{>0}), \quad [T(a,b)] \xrightarrow{\tau'} [a,b]. \tag{21}$$

In the other direction, it is clear that $\tau\tau' = \mathsf{id}$. Consequently, the homomorphism τ in (20) is an isomorphism. □

Extending from $\mathbb{R}_{>0}$ to $\mathbb{R}$ and adding bilinearity relations on the symbols $[a,b]$, so that, in addition $[a_1+a_2,b] = [a_1,b]+[a_2,b]$, gives a surjective homomorphism

$$\theta' \ : \ Z^2(\mathbb{R}_{>0}) \longrightarrow \mathbb{R} \wedge_{\mathbb{Z}} \mathbb{R} \cong \mathbb{R} \wedge_{\mathbb{Q}} \mathbb{R}, \tag{22}$$

and, consequently, a surjective homomorphism

$$\theta \ : \ \mathsf{Cob}^{1,\mathsf{up}}_{\mathbb{R}_{>0}} \longrightarrow \mathbb{R} \wedge_{\mathbb{Q}} \mathbb{R} \tag{23}$$

taking $[T(a,b)]$ to $a \wedge b$ (compare with the SAF invariant, see Section 2). This allows to show that some unoriented planar 1-foams are not null-cobordant.

Corollary 3.4. Planar unoriented foam $T(a,b)$ for $a,b \in \mathbb{R}_{>0}$ is not null-cobordant if $b \notin \mathbb{Q}a$.

That is, if the unoriented planar foam $T(a,b)$ for $a,b \in \mathbb{R}_{>0}$ is null-cobordant, then $b \in \mathbb{Q}a$.

It turns out that the bracket $[a,b]$ is almost bilinear, as explained by the following result.

Proposition 3.5. The kernels of θ' and θ consist of elements of order at most two. For any $a, b_1, b_2 \in \mathbb{R}_{>0}$ the following relation holds in $Z^2(\mathbb{R}_{>0})$:

$$2([a, b_1 + b_2] - [a, b_1] - [a, b_2]) \;=\; 0. \tag{24}$$

Proof. Consider the following three equations:

$$[a, b_1 + b_2] + [b_1, b_2] \;=\; [a + b_1, b_2] + [a, b_1], \tag{25}$$

$$[b_1, b_2 + a] + [b_2, a] \;=\; [b_1 + b_2, a] + [b_1, b_2], \tag{26}$$

$$[b_1, a + b_2] + [a, b_2] \;=\; [a + b_1, b_2] + [b_1, a]. \tag{27}$$

Equation (25) is the 2-cocycle relation, for a, b_1, b_2. Equation (26) is given by cyclicly permuting the terms of the previous equation, $a \longmapsto b_1 \longmapsto b_2 \longmapsto a$. Equation (27) is given by transposing a and b_1 in (25). Writing down the linear combination (25) + (26) − (27) and using that the bracket is antisymmetric gives relation (24).

This argument is borrowed from [5], which shows bilinearity of the difference $[a,b] - [b,a]$ assuming only the 2-cocycle equation (16) for all $a, b \in H$, where H is an abelian group. When the 2-cocycle is, additionally, antisymmetric, via equation (15), the difference $[a,b] - [b,a] = 2[a,b]$. □

The proposition tells us that the bracket $[a,b]$ is "almost" bilinear, with the difference $[a, b_1 + b_2] - [a, b_1] - [a, b_2]$ either 0 or an element of order 2.

Corollary 3.6. The foam $U \sqcup U$, where

$$U \;=\; T(a, b_1 + b_2) \sqcup T(b_1, a) \sqcup T(b_2, a),$$

is null-cobordant for any $a, b_1, b_2 > 0$.

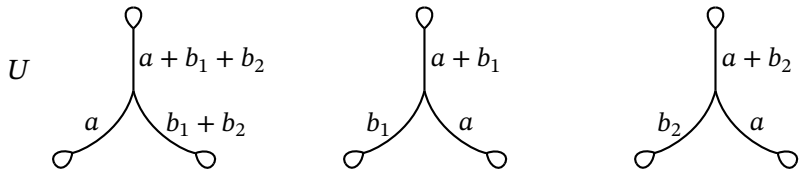

Figure 30: The 1-foam $U = T(a, b_1 + b_2) \sqcup T(b_1, a) \sqcup T(b_2, a)$ in Corollary 3.6.

The foam U is shown in Figure 30.

We do not know whether the scalar 2 can be dropped from equation (24), so that $[a, b]$ is bilinear in a, b. That would be equivalent to foams U in Corollary 3.6 being null-cobordant for all $a, b_1, b_2 > 0$.

To further study abelian groups in Proposition 3.3, it is natural to extend the possible weights of the foam facets from positive to all real numbers. First, we discuss the group $Z^2(H)$ for general commutative semigroups H, having $(\mathbb{R}, +)$ in mind. Note that Proposition 3.5 holds for any commutative semigroup H in place of $\mathbb{R}_{>0}$, so that there is an exact sequence

$$0 \longrightarrow \ker \theta' \longrightarrow Z^2(H) \xrightarrow{\theta'} H \wedge' H \longrightarrow 0,$$

with $2x = 0$ for $x \in \ker \theta'$. Here $H \wedge' H$ is the abelian group which is the quotient of the abelian group closure of $H \otimes_{\mathbb{Z}} H$ by the relations $a \wedge' b + b \wedge' a = 0$ and $a \wedge' a = 0$, by analogy with (14), (15). Symbol $\wedge'$ is used instead of $\wedge$ since the relation $a \wedge a = 0$ is usually not imposed in the definition of the exterior square (but follows for 2-divisible semigroups).

If $0 \in H$, then (16) with the particular triple $(a, b, c) = (a, 0, b)$ implies that $[a, 0] = [0, b]$ for all $a, b \in H$. Specializing to $b = 0$ gives

$$[a, 0] \;=\; [0, a] \;=\; 0, \; \forall a \in H. \tag{28}$$

Proposition 3.7. Assume that $0 \in H$. Then

1. $[a, 0] = 0$ for all $a \in H$,

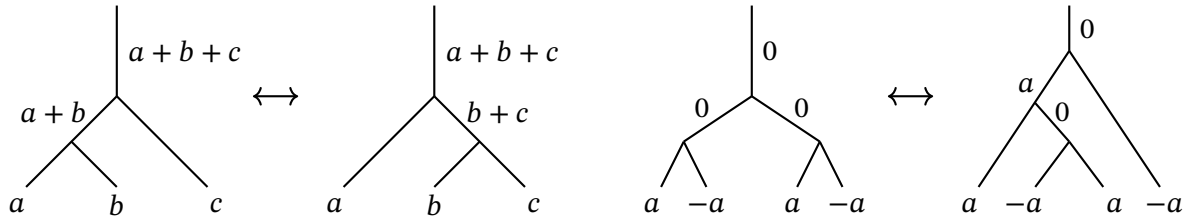

Figure 31: Left: cobordance of these 1-foams matches the 2-cocycle equation (16). Right: Two trees merging $(a, -a, a, -a)$ to 0.

2. If $-a \in H$ (i.e., a is invertible in H), then

$$2[a, -a] = 0, \tag{29}$$

$$[b, -a] = [a, b - a] + [a, -a] \text{ for all } b \in H, \tag{30}$$

$$[2a, -2a] = 0, \tag{31}$$

3. If $-a, -b \in H$, then

$$[-a, -b] = [a, b] + [a, -a] + [b, -b] - [a + b, -a - b]. \tag{32}$$

Proof. See (28) for 1. Notice that relation (16) can be visualized as the "associativity" property for merging a, b, c into $a + b + c$ in two possible ways, where a vertex merging x, y contributes $[x, y]$ to the sum, see Figure 31.

Iterating this associativity relation gives us a relation between any two tree diagrams for merging $(a_1, \dots, a_n)$ into $a_1 + \dots + a_n$. Now apply the relation to the two trees shown in Figure 31 on the right merging $(a, -a, a, -a)$ to 0 and use that $[a, -a] + [-a, a] = 0$ and $[b, 0] = 0$ for any b to conclude that $2[a, -a] = 0$, resulting in relation (29).

For the relation (30), apply (16) to $(b-a, a, -a)$ to get $[b-a, a]+[b, -a] = [b-a, 0]+[a, -a]$. For the relation (31), two of the ways to merge $(a, a, -a, -a)$ to 0 give

$$[a, a] + [-a, -a] + [2a, -2a] = [a, -a] + [a, 0] + [a, -a], \tag{33}$$

resulting in $[2a, -2a] = 2[a, -a] = 0$.

For the relation (32), apply (16) to $(a, -a, -b)$ and $(-a - b, a, b)$. □

Notice that, modulo terms $[x,-x]$, relations (30) and (32) are $[b,-a]\sim[a,b-a]$ and $[-a,-b]\sim[a,b]$.

Remark 3.8. We give an example for which $[a,-a]\neq 0$. Let $H=(\mathbb{Z}/4,+)=\{0,1,2,3\}$. It is tedious but straightforward to check that the map

$$\psi([a,b])=\begin{cases}0 & \text{if } a=0 \text{ or } b=0 \text{ or } a=b,\\ 1 & \text{otherwise}\end{cases} \tag{34}$$

extends to a homomorphism $\psi : Z^2(\mathbb{Z}/4)\longrightarrow \mathbb{Z}/2$. Under this homomorphism, the image of $[1,-1]=[1,3]$ is nontrivial. Via the surjective homomorphism $\mathbb{Z}\longrightarrow\mathbb{Z}/4$ we see that $[1,-1]$ in nontrivial in $Z^2(\mathbb{Z})$ as well. Consequently, $[a,-a]$ is not always 0 in $Z^2(H)$ for $a,-a\in H$.

Elements $[a,-a]$, over all $a,-a\in H$, generate a 2-torsion subgroup in $Z^2(H)$, which we can denote $Z^2_{-}(H)$. This subgroup is trivial if H is 2-divisible, in view of the relation (31). In particular, it is trivial for $H=(\mathbb{R},+)$.

We denote by $\mathbb{R}_{>0}$ the semigroup $(\mathbb{R}_{>0},+)$ and by $\mathbb{R}$ the group $(\mathbb{R},+)$. Semigroup $(\mathbb{R}_{>0},+)$ is not a monoid, that is, $0\notin\mathbb{R}_{>0}$. The inclusion $\mathbb{R}_{>0}\subset\mathbb{R}$ induces a homomorphism

$$\rho \ : \ Z^2(\mathbb{R}_{>0})\longrightarrow Z^2(\mathbb{R}). \tag{35}$$

To differentiate between the elements of the two groups, denote by $[a,b]_{\mathbb{R}}$ the symbol of the pair $a,b\in\mathbb{R}$ viewed as an element of $Z^2(\mathbb{R})$. The map ρ is given by $\rho([a,b])=[a,b]_{\mathbb{R}}$ for $a,b>0$.

Corollary 3.9. In $Z^2(\mathbb{R})$ and for $a,b>0$, the following relations hold:

$$[a,-b]_{\mathbb{R}}=\begin{cases}[b,a-b]_{\mathbb{R}} & \text{if } a>b,\\ [b-a,a]_{\mathbb{R}} & \text{if } a<b,\\ 0 & \text{if } a=b,\end{cases} \tag{36}$$

$$[-a,b]_{\mathbb{R}}=-[b,-a]_{\mathbb{R}},\quad [-a,-b]_{\mathbb{R}}=[a,b]_{\mathbb{R}}. \tag{37}$$

Proof. These relations are obtained by dropping off the terms $[x,-x]$ from the relations in Proposition 3.7. Terms $[x,-x]_{\mathbb{R}}=0$ since $\mathbb{R}$ is 2-divisible. □

Corollary 3.9 implies that ρ is surjective, since the symbol $[a,b]_{\mathbb{R}}$ with at least one of a,b negative can be written as $\pm\rho([a',b'])$ for suitable $a',b'\in\mathbb{R}_{>0}$, or $[a,b]_{\mathbb{R}}=0$.

Proposition 3.10. The homomorphism

$$\rho \ : \ Z^2(\mathbb{R}_{>0}) \longrightarrow Z^2(\mathbb{R})$$

induced by the inclusion $\mathbb{R}_{>0}\subset\mathbb{R}$ is an isomorphism.

Proof. Corollary 3.9 relations can be used to define a map from symbols $[a,b]_{\mathbb{R}}$ with $a,b\in\mathbb{R}$ to signed symbols $[a,b]$ with positive a,b. Consider the map δ defined on symbols as follows and assuming $a,b>0$:

$$\delta([a,b]_{\mathbb{R}}) = \delta([-a,-b]_{\mathbb{R}}) = [a,b], \tag{38}$$

$$\delta([a,-b]_{\mathbb{R}}) = [b,a-b], \text{ if } a>b, \tag{39}$$

$$\delta([a,-b]_{\mathbb{R}}) = [b-a,a], \text{ if } a<b, \tag{40}$$

$$\delta([-a,b]_{\mathbb{R}}) = -\delta([b,-a]_{\mathbb{R}}), \tag{41}$$

$$\delta([a,-a]_{\mathbb{R}}) = 0. \tag{42}$$

We claim that δ extends to a well-defined homomorphism $\delta \ : \ Z^2(\mathbb{R}) \longrightarrow Z^2(\mathbb{R}_{>0})$. This map respects the relations (14) and (15). A tedious case-by-case verification shows that it also respects the relation (16). For example, consider relation (16) for the triple $(a,-b,c)$ where $c>b>a>0$. To check that

$$\delta([a,-b]_{\mathbb{R}})+\delta([a-b,c]_{\mathbb{R}})=\delta([a,c-b]_{\mathbb{R}})+\delta([-b,c]_{\mathbb{R}}),$$

we compute the two sides:

$$\mathrm{LHS} = [b-a,a]+[a+c-b,b-a],$$

$$\mathrm{RHS} = [a,c-b]+[c-b,b],$$

and write

$$\begin{aligned}[a,c-b]+[c-b,b] &= ([c-b,b]+[a,b-a])+[a,b-c]-[a,b-a]\\ &= ([c-b,a]+[a+c-b,b-a])+[a,b-c]-[a,b-a]\\ &= [a+c-b,b-a]+[b-a,a] \;=\; \mathsf{LHS}.\end{aligned}$$

The case $a>b>c$ follows by symmetry, and other cases to consider are $a>b, c>b$; $b>a+c$; $a+c>b, b>a, b>c$. All of them together take care of the relation (16) when only the middle number is negative. The case $(-a,-b,-c)$, i.e., all three numbers are negative, is trivial, but there are many other cases. They follow via straightforward computations which are omitted. □

The group $Z^2(H)$ depends only on the isomorphism class of abelian semigroup H. Thinking of $\mathbb{R}$ an abelian group and using the axiom of choice, one can write $\mathbb{R}\cong\oplus_J\mathbb{Q}$, where the index set J is uncountable. Consequently, $Z^2(\mathbb{R}_{>0})\cong Z^2(\mathbb{R})\cong Z^2(\oplus_J\mathbb{Q})$, giving a more symmetric presentation of $Z^2(\mathbb{R}_{>0})$ since we can now work with positive and *non-positive* generators satisfying the relations (14) - (16). This does not give an explicit description of $Z^2(\mathbb{R}_{>0})$, just a description with more internal symmetries, but in our study of this group we stop here. A natural question would be to understand the kernel of the surjective homomorphism $\theta' : Z^2(\mathbb{R}_{>0})\longrightarrow \Lambda^2_{\mathbb{Q}}(\mathbb{R})$ sending $[a,b]$ to $a\wedge b$. From Proposition 3.5 we know that $2x=0$ for any element $x\in\ker(\theta')$.

Remark 3.11. Note that $Z^2(\mathbb{Q}_{>0})\cong Z^2(\mathbb{Q})=0$. This can be derived from all tripods $T(a,b)$ for $a,b\in\mathbb{Q}_{>0}$ being null-homotopic. A related observation is that thickening $T(a,b)$ with rational a,b results in a foliated planar surface with all leaves closed and diffeomorphic to $\mathbb{S}^1$.

Proposition 3.10 shows that passing from $\mathbb{R}_{>0}$ to $\mathbb{R}$ does not change the group Z^2. Let us consider unoriented planar 1-foams where edges are labeled by real numbers rather than just positive numbers (planar $\mathbb{R}$-weighted 1-foams). A cobordism between two such foams is given by an unoriented $\mathbb{R}$-decorated 2-foam in $\mathbb{R}^2\times[0,1]$. An $\mathbb{R}$-weighted 2-foam

Figure 32: Going from an $\mathbb{R}$-weighted 1-foam to an $\mathbb{R}_{\geq 0}$-weighted 1-foam (continues in Figures 33, 34).

also has vertices with local structure as in Figures 7 and 5, but now a, b, c are arbitrary real numbers, possibly 0. Denote by $\mathsf{Cob}^{1,\mathrm{up}}_{\mathbb{R}}$ the cobordism group of $\mathbb{R}$-weighted planar unoriented 1-foams. There is a natural homomorphism

$$\iota \ : \ \mathsf{Cob}^{1,\mathrm{up}}_{\mathbb{R}_{>0}} \longrightarrow \mathsf{Cob}^{1,\mathrm{up}}_{\mathbb{R}} \tag{43}$$

given by viewing $\mathbb{R}_{>0}$-weighted 1- and 2-foams as $\mathbb{R}$-weighted foams. Likewise, there is a homomorphism

$$\tau_{\mathbb{R}} \ : \ Z^2(\mathbb{R}) \longrightarrow \mathsf{Cob}^{1,\mathrm{up}}_{\mathbb{R}} \tag{44}$$

defined analogously to the homomorphism (20). The map $\tau_{\mathbb{R}}$ takes the symbol $[a,b]_{\mathbb{R}}$ to the concordance class of the tripod $T(a,b)$, where now the weights may be non-positive.

Theorem 3.12. Maps ι and $\tau_{\mathbb{R}}$ are isomorphism of abelian groups.

Proof. That $\tau_{\mathbb{R}}$ is an isomorphism can be shown in the same way as for τ, see the proof of Proposition 3.3. Next, observe that formulas in Corollary 3.9 convert symbols $[x,y]_{\mathbb{R}}$ when one of both x, y are negative into symbols with positive entries. We now define the foam counterpart of these formulas. Start with an $\mathbb{R}$-weighted 1-foam U and convert it to an $\mathbb{R}_{\geq 0}$-weighted 1-foam U° as follows. First, convert each line a into a line of weight $|a|$, for $a \in \mathbb{R}^*$, see Figure 32.

At the vertices of U, only the edges of *negative* weight are bent to the opposite side to retain the balance of weights at a vertex. If an edge has positive weight, it is not bent. Figure 33 shows how a single negative edge is bent at a vertex. Figure 34 shows modifications at a vertex if two out of three edges have negative weights. In Figure 35

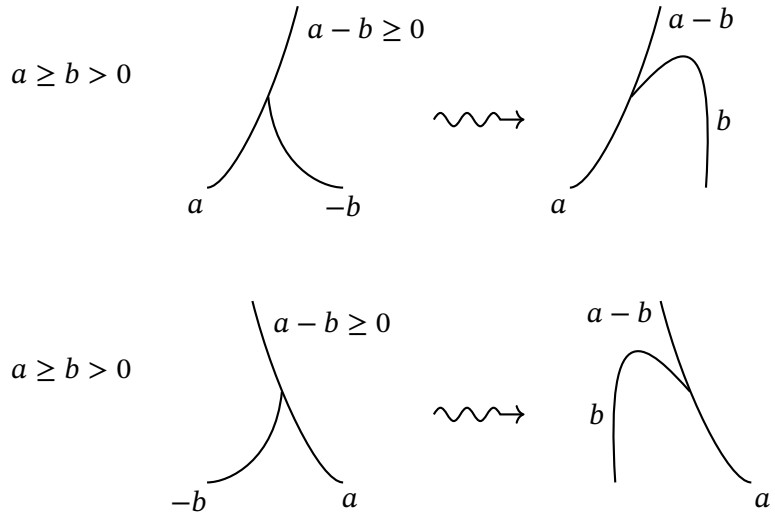

Figure 33: Converting a vertex with one negative weight into a positive vertex; compare with (36), top equality. If $a = b$, the line $a - b = 0$ is removed, see also Figure 35.

top row, we see that an $(a, -a)$ vertex gets smoothed out into part of a segment, and in Figure 35 bottom row, that no bending is necessary at a $(-a, -b)$ vertex, but just weight reversal at all three edges of the vertex.

The foam U° may have edges (and circles) of weight 0. A circle of any weight is null-cobordant even if there is a 1-foam inside the disk that it bounds, by converting the circle to a barbell. Given a 0-edge e, applying Figure 26 (left) transformation at the two endpoints of e produces tripod foams $T(a_1, 0)$ and $T(a_2, 0)$ (or their reflections) for some

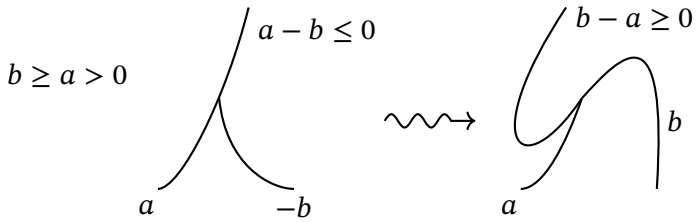

Figure 34: Vertex replacement when two out of three edges are negative. If $a = b$, the line $b - a = 0$ is erased.

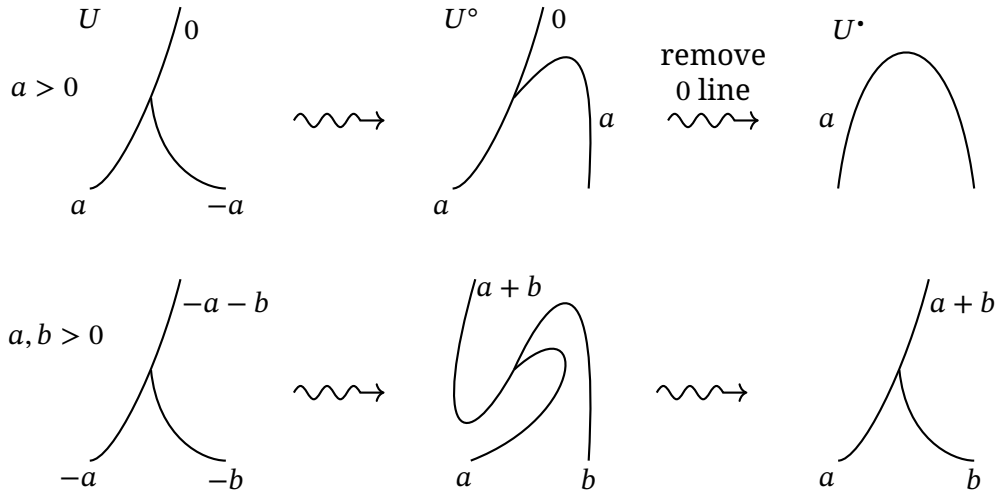

Figure 35: Top row: converting $(a, -a)$-vertex to an undecorated a-segment (analogous to the relation $[a, -a]_{\mathbb{R}} = 0$) by flipping (bending) the $-a$ edge and removing the 0 edge. Bottom row: at a $(-a, -b)$-vertex, all edges are negative so one bends all three edges or one simply reverses all weights (corresponding to the relation $[-a, -b]_{\mathbb{R}} = [a, b]_{\mathbb{R}}$, see Corollary 3.9).

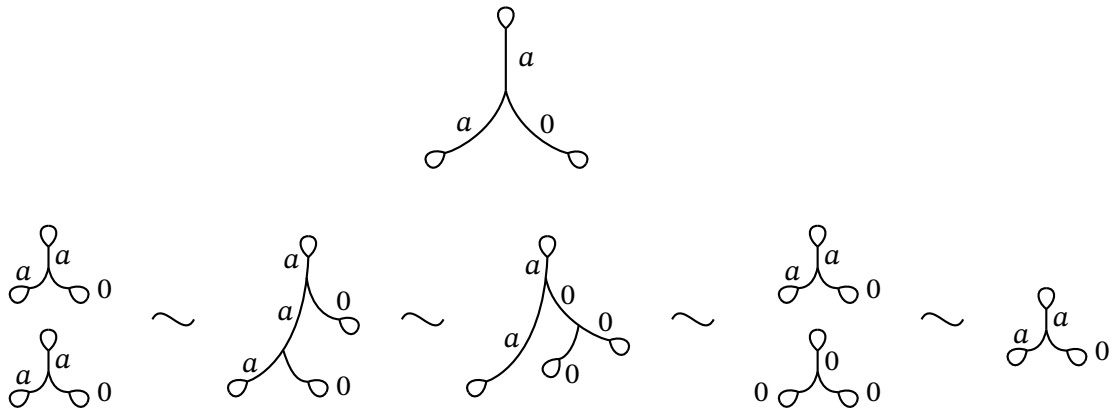

Figure 36: Top: $T(a,0)$ tripod. Bottom row: a cobordism from $T(a,0) \sqcup T(a,0)$ to $T(a,0)$. The first move is the cobordism in Figure 24, the second is $(a,0,0)$-vertex, the third move cuts a 0 edge creating lollipops. The last move vanishes $T(0,0)$, since it is null-cobordant. Gluing $T(a,0) \times [0,1]$ to this cobordism by capping off one $T(a,0)$ on each side shows that $T(a,0)$ is null-cobordant.

a_1, a_2. These foams are null-cobordant (see Figure 36), and cobordant to barbell foams with weights a_1, a_2 (the latter are null-cobordant as well, see Figure 27). Inserting these barbell foams back into the original 1-foam and composing these cobordisms shows that an $\mathbb{R}_{\geq 0}$-weighted 1-foam V with a 0-weight edge e is cobordant to the same foam with edge e deleted. Thus, all edges and circles of weight 0 (components of weight 0) can be deleted from an $\mathbb{R}_{\geq 0}$-weighted foam V, resulting in a cobordant $\mathbb{R}_{>0}$-foam. In particular, this is shown as the second step in the top row of Figure 35.

Denote by $U^\bullet$ the foam U° with weight 0 components removed. The map $U \longmapsto U^\bullet$ from planar $\mathbb{R}$-weighted 1-foams to planar $\mathbb{R}_{>0}$-weighted 1-foams needs to be extended to cobordisms between 1-foams, that is, to 2-foams with boundary.

Suppose that F is an $\mathbb{R}$-weighted 2-foam with boundary U, unoriented and embedded in $\mathbb{R}^2 \times [0,1)$, with $U \cong \partial F \cong F \cap (\mathbb{R}^2 \times \{0\})$. We convert all facets of F with negative labels $-a$ to positive labels $a > 0$.

At each seam of F, two facets merge into one. If one or two of these facets had negative

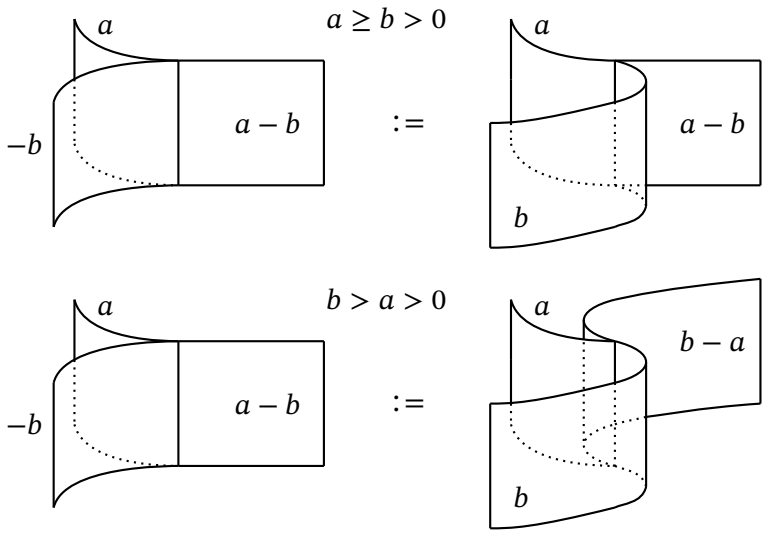

Figure 37: Top row: Converting a seam with a, $-b$ thin facets, with $a \geq b > 0$, into a seam with b, $a-b$ thin facets. Bottom row: Converting a seam when $b > a$.

weights, we make these facets approach the seams from the opposite side, by taking the rules in Figures 33, 34, 35 and multiplying them by the interval to get the corresponding rules for 2-foams. These modifications are depicted in Figure 37.

Next, one produces modification rules at vertices of F, where facets have weights $a, b, c, a+b, b+c, a+b+c$, for some $a, b, c \in \mathbb{R}$. Taking the link of a vertex results in a 2-foam $L(a,b,c)$ on the 2-sphere (see Figure 8 on the left, with orientations and thin edge orders at nodes dropped). Converting it to $L(a,b,c)^{\bullet}$, one needs to check that it is null-cobordant through a $\mathbb{R}_{>0}$-weighted foam and pick a particular cobordism to replace each (a,b,c)-vertex of an $\mathbb{R}$-weighted 2-foam. This is done on a case-by-case basis, and the rest of the proof closely resembles that of Proposition 3.10 towards the end. Here we provide the cobordisms in two out of the many cases here. Instead of the cobordism from $L(a,b,c)^{\bullet}$ to the empty foam we depict cobordisms between two possible ways to merge a, b, c edges into the $a+b+c$ edge, see Figure 26 on the right.

We consider the case when the middle number is negative and write it as $-b$. Since intermediate edges are $a-b$ and $c-b$, there are four cases to consider:

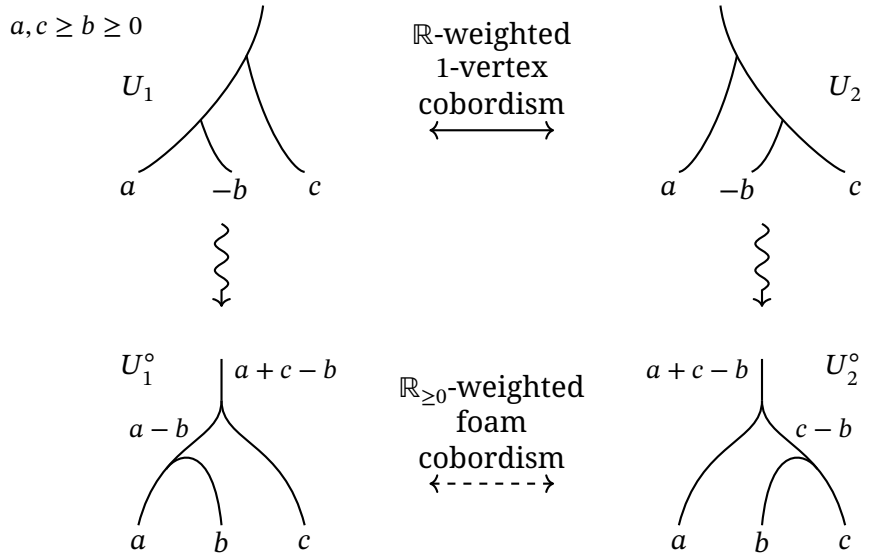

Figure 38: Vertical arrows go from $\mathbb{R}$-weighted foams U_1, U_2 to $\mathbb{R}_{\geq 0}$-weighted foams U_1°, U_2°. Bottom horizontal arrow indicates that we need to produce an $\mathbb{R}_{\geq 0}$-weighted cobordism between foams U_1°, U_2°. Such a cobordism is shown in Figure 39.

1. $a \geq b, c \geq b \geq 0$,
2. $a \geq b \geq c \geq 0$ (case $c \geq b \geq a \geq 0$ is given by reflection),
3. $b \geq a, b \geq c, a + c \geq b$, $a, c \geq 0$,
4. $b \geq a + c$, $a, c \geq 0$.

In each of the cases, one constructs an $\mathbb{R}_{>0}$-weighted cobordism between the corresponding $\mathbb{R}_{>0}$-weighted one foams. Schematically, Figure 38 shows what needs to be done in case (1) above, and similar for the other cases.

Cobordisms between the diagrams that replace the corresponding vertices are shown for cases (1) and (3) in Figures 39 and 40 via sequences of their cross-sections.

Further cases include $L(-a, b, c)$, with the first number negative (that of $L(a, b, -c)$ follows by reflection symmetry). Another case is when two numbers out of three are

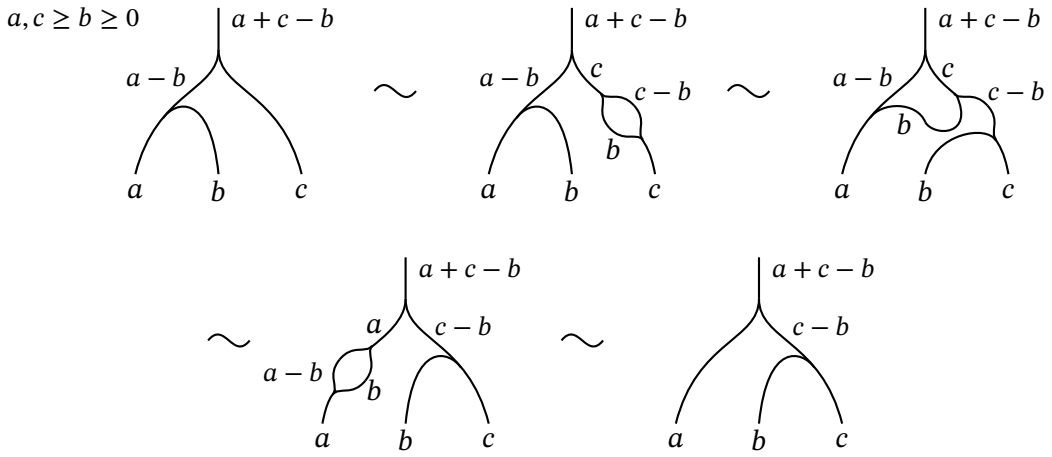

Figure 39: Replacing a vertex of an $\mathbb{R}$-weighted 2-foam for weights $(a, -b, c)$ with $a, c \geq b \geq 0$ by an $\mathbb{R}_{\geq 0}$-weighted 2-foam.

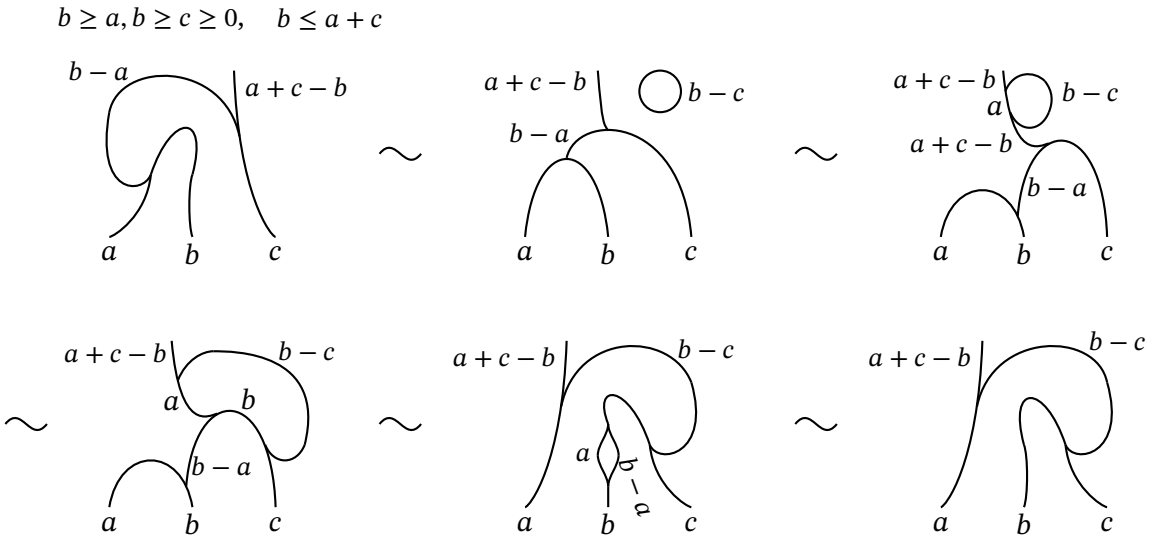

Figure 40: Vertex replacement for weights $(a, -b, c)$ with $b \geq a, b \geq c \geq 0$ and $b \leq a + c$.

negative. The case $L(-a,-b,-c)$ is easy, since no modifications are done at any of the four vertices of the boundary foam. (It is likely that additional symmetries of $L(a,b,c)^\bullet$ can be used to reduce the number of cases but we have not checked that.)

This procedure converts $\mathbb{R}$-weighted 2-foam F with boundary $U \cong \partial F$ to an $\mathbb{R}_{\geq 0}$-weighted embedded foam, denoted F°, with boundary U°.

Next, 0-facets of F° can be removed as well, by analogy and extending our deletion of 0-facets of the foam U°. The resulting 2-foam $F^\bullet \subset \mathbb{R}^2 \times [0,1)$ is $\mathbb{R}_{>0}$-weighted, with the boundary $U^\bullet \subset \mathbb{R}^2 \times \{0\}$. Consequently, our procedure for converting $\mathbb{R}$-weighted 1- and 2-foams into $\mathbb{R}_{>0}$-weighted 1- and 2-foams gives a homomorphism

$$\iota^\bullet \ : \ \mathsf{Cob}^{1,\mathsf{up}}_{\mathbb{R}} \longrightarrow \mathsf{Cob}^{1,\mathsf{up}}_{\mathbb{R}_{>0}}.$$

It is clear that $\iota^\bullet \circ \iota = \mathsf{id}$, since $\iota^\bullet$ on foams with all facets positive is the identity map.

To show that $\iota \circ \iota^\bullet = \mathsf{id}$ it suffices to check that ι is surjective. For that, it is enough to show that $[T(a,b)]$ is in the image of ι for all $a,b \in \mathbb{R}$. Consider the tripod $T(a,-b)$ for $a \geq b \geq 0$. There are two ways to merge strands $a,-b,b$ into an $a-b+b=a$ strand, with the one-vertex 2-foam cobordism connecting the two ways to merge. This translates into a cobordism between $\mathbb{R}$-weighted 1-foams:

$$T(a,-b) \sqcup T(a-b,b) \sim T(a,0) \sqcup T(-b,b).$$

Foam $T(a-b,b)$ has positive weights. Foam $T(a,0)$ is null-cobordant via $\mathbb{R}_{\geq 0}$-weighted foams, see Figure 36. Foam $T(-b,b)$ is null-cobordant, since $[-b,b]_{\mathbb{R}} = 0$ and $[T(-b,b)]$ is the image of $[-b,b]_{\mathbb{R}}$ under the homomorphism $\tau_{\mathbb{R}}$ in (44). Alternatively, computation in (33) with $-b/2$ in place of a can be converted into a description of a cobordism from $T(-b,b)$ to the empty 1-foam. Consequently, $T(a,-b)$ is cobordant via an $\mathbb{R}$-weighted 2-foam to an $\mathbb{R}_{>0}$-weighted 1-foam $T(b,a-b)$. Reflecting in the plane shows that $T(-b,a)$ is cobordant to $T(a-b,b)$. We leave the remaining cases: $T(a,-b)$ with $b>a>0$ and $T(-a,-b)$, $a,b>0$ to the reader.

Consequently, ι and $\iota^\bullet$ are mutually-inverse isomorphisms. This completes the proof of Theorem 3.12. □

Our constructions and results can be summarized into the following statement.

Theorem 3.13. There is a commutative diagram of isomorphisms of abelian groups

$$\begin{array}{ccc} Z^2(\mathbb{R}_{>0}) & \xrightarrow{\tau} & \mathsf{Cob}^{1,\mathrm{up}}_{\mathbb{R}>0} \\ \downarrow{\scriptstyle \rho} & & \downarrow{\scriptstyle \iota} \\ Z^2(\mathbb{R}) & \xrightarrow{\tau_{\mathbb{R}}} & \mathsf{Cob}^{1,\mathrm{up}}_{\mathbb{R}} \end{array} \tag{45}$$

The top arrow is given by (20), the bottom arrow $\tau_{\mathbb{R}}$ is the map (44). The left arrow is the map ρ in Proposition 3.10, the right arrow is given by (43).

In particular, the cobordism groups of $\mathbb{R}$-weighted and $\mathbb{R}_{>0}$-weighted planar unoriented 1-foams are isomorphic, and they are isomorphic to the corresponding abelian groups generated by the symbols $[a, b]$ over either all positive real $a, b > 0$ or, alternatively, all real a, b, subject to relations (14) - (16) in each of the two cases.

Remark 3.14. In the isomorphisms τ or $\tau_{\mathbb{R}}$ in Theorem 3.13, commutative semigroup $\mathbb{R}_{>0}$ or commutative group $\mathbb{R}$ can be replaced by any uniquely 2-divisible commutative semigroup H or by a semimodule over $\mathbb{Z}_{>0}[1/2]$. Unique 2-divisibility is needed to consistently split a planar H-weighted 1-foam into a union of tripods, since lollipop loops carry weights $a/2, b/2, (a+b)/2$. These divisions by two must exist and be consistent. One then gets an isomorphism of abelian groups

$$\mathsf{Cob}^{1,\mathrm{up}}_{H} \cong Z^2(H). \tag{46}$$

The group $Z^2(H)$ can be thought of as a universal *antisymmetric* 2-cocycle on H. Antisymmetry condition forces the bracket to be almost bilinear, see Proposition 3.5.

Symmetric 2-cocycles are not almost bilinear, in this sense, and allow for a richer structure. Interestingly, they naturally appear in the theory of formal groups [32, Section 6], with relations (16) and $[a, b] = [b, a]$ interpreted as the infinitesimal version of the formal group law axioms. Formal groups are closely related to cobordism groups of manifolds (to the complex cobordism generalized cohomology theory), see [1, 21, 26, 31, 10] and the references therein.

It seems possible to interpret symmetric 2-cocycles in the framework of foam cobordisms. A step towards such interpretation is to consider unoriented cobordisms (2-foams with boundary) between 1-foams, not embedded anywhere, where 2-foams have oriented seams. One imposes the compatibility condition on seam orientations at vertices of the 2-foam to match the 2-cocycle relation. Absence of an embedding and not keeping track of the order of thin facets at a seam leads to the symmetric relation $[a,b]=[b,a]$. The antisymmetry property vanishes, since in the cobordisms in the top row of Figure 16 the seams are now oriented and the two vertices of the boundary 1-foam for each relation have opposite types, leading us to denote the two brackets by $[a,b]_+$ and $[a,b]_-$ and giving the relation $[a,b]_+ + [b,a]_- = 0$, which simply allows to express one bracket via the other. The bracket $[a,b]_+$, then, satisfies the symmetry property and the 2-cocycle condition.

Remark 3.15. For an interesting cobordism group, we considered planar *unoriented* weighted 1-foams in this section. The planar *oriented* 1-foams do not allow loops and creation of tripod foams $T(a,b)$. The cobordism group of suitably defined planar oriented 1-foams is trivial.

Constructions and results of this section demonstrate the possibility of having interesting cobordism groups of planar objects other than embedded 1-manifolds, with additional decorations, such as (positive) real weights. Notice that the resulting cobordism group has the flavour of scissor congruence groups (for instance, surjecting onto $\Lambda^2_{\mathbb{Q}}\mathbb{R}$, so that $\mathbb{R}$ is essentially viewed as a discrete group, which is typical of scissor congruence).

4 Variations on weighted foams

Here we go back to considering oriented $\mathbb{R}_{>0}$-weighted foams, not embedded anywhere, as in Section 2.

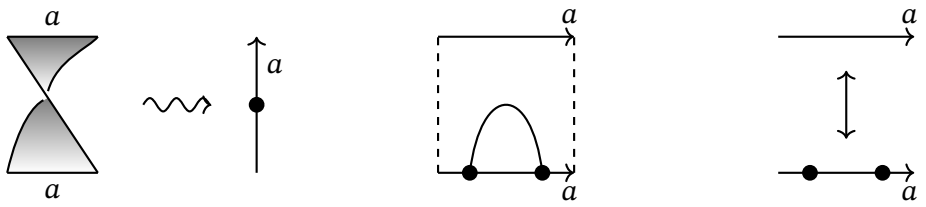

Figure 41: Left: encoding flip by a dot. Middle: a cobordism that cancels a pair of dots on a line. Right: Removing or adding two dots on a line results in a cobordant foam. Our surfaces are not embedded in $\mathbb{R}^3$, and the square of the flip is the identity.

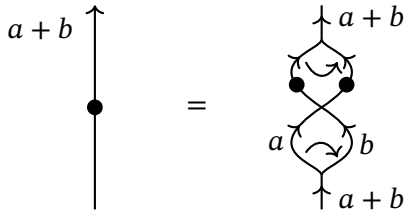

Figure 42: Splitting an $(a+b)$-line flip into a-line and b-line flips.

4.1 Foams with flips

The group of IET automorphisms of the interval can be enhanced with flips $[0,a] \longrightarrow [0,a], x \longmapsto a - x$, see [19], viewed as a subgroup of all measurable automorphisms of $([0,1],|dx|)$. Denote this automorphism group by G_{flip}; it contains $\mathsf{Aut}_{\mathsf{IET}}$ as a subgroup. Arnoux in [3, 4], also see [19], has shown that this group is simple, in particular, $[G_{\mathsf{flip}}, G_{\mathsf{flip}}] = G_{\mathsf{flip}}$.

A flip of an interval $[0,a]$ can be encoded by a dot on a line labeled a, see Figure 41. IET 1-foams and 2-foams can be enhanced by flip dots and flip networks, subject to the following relations:

- Two dots on an interval can cancel via a cobordism,
- A flip line on an $(a+b)$-facet can cross a seam and become two flip lines on a, b facets, reversing the order of the two thin facets at the seam,

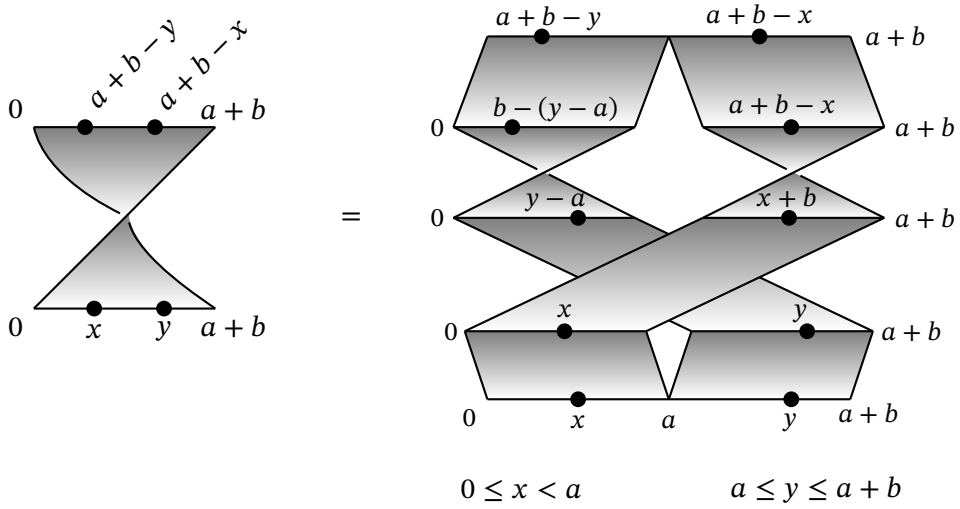

Figure 43: The flip map $x \longmapsto 1 - x$ can be split as shown on the right.

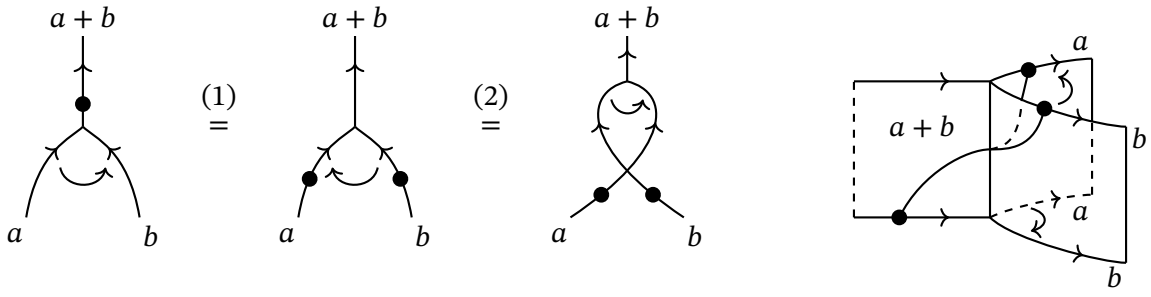

Figure 44: Equation (1) encodes moving a dot through a vertex, which includes flipping the order of thin edges. Relation (2) follows from Move 4 in Figure 15, which does not involve dots. Right: foam cobordism between the two foams in equation (1), with reversed orientation. Here, the direction is reversed during the interaction.

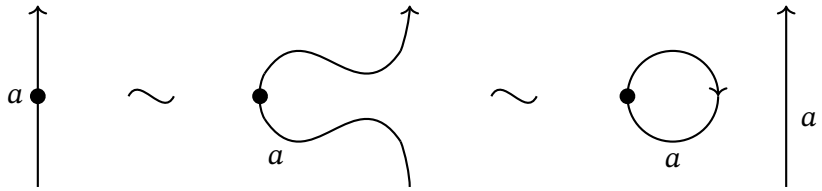

Figure 45: Splitting a dot off the rest of the foam.

as shown in Figures 41 and 44. Figure 42 shows how a flip on an $(a+b)$-line is modified to flips on a- and b-lines, via a concordance of braid-like 1-foams with flips. Figure 43 shows the thickened version of that equivalence transformation. Denote by $\mathsf{Cob}^{1,\mathsf{flip}}_{>0}$ the cobordism group of $\mathbb{R}_{>0}$-decorated 1-foams with flips.

Theorem 4.1. The cobordism group of weighted oriented 1-foams with flips is trivial,

$$\mathsf{Cob}^{1,\mathsf{flip}}_{>0} \;\cong\; 0. \tag{47}$$

Proof. Any $\mathbb{R}_{>0}$-decorated 1-foam with flips U can be represented as the closure $\widehat{U}_0$ of a braid-like foam U_0. To U_0 there is associated the corresponding element $u_0 \in G_{\mathsf{flip}}$. Since G_{flip} is perfect, u_0 can be represented as a product of commutators, $u_0 = \prod_{i=1}^{k}[v_i, w_i]$. Write U_0 as the composition of corresponding 1-foams, $U_0 = \prod_{i=1}^{k}[V_i, W_i]$. The foam for each commutator is cobordant to the interval foam, using the argument as in Figure 12. Consequently $[U] = 0$ in the cobordism group. □

Remark 4.2. Theorem 4.1 can also be proved directly, without invoking the perfectness of G_{flip}. Start with a 1-foam U, possibly with flips. A dot can be split off from the rest of U into an a-circle with a dot, see Figure 45. An a-circle with a dot is null-cobordant, see Figure 46.

Consequently, a 1-foam with flips is cobordant to the same foam without flips, and flips can be removed at any time when constructing a sequence of cobordisms. Present foam U as the closure of a braid-like foam U_0. All crossings in U_0 can be split off from a diagram as in Figure 18, along with the flips.

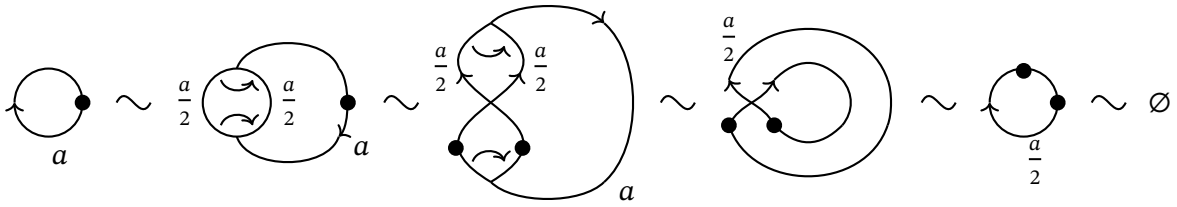

Figure 46: An a-circle with a dot is null-cobordant.

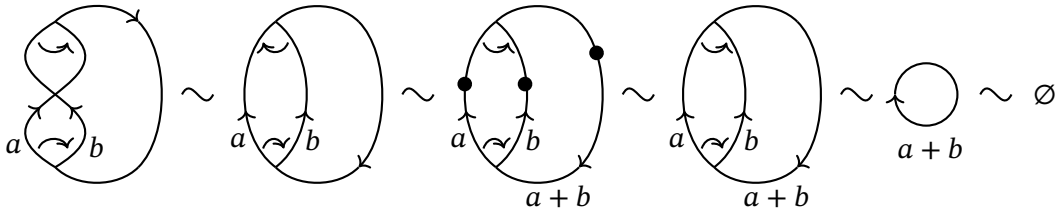

Figure 47: A cobordism from $U_{a,b}$ to the empty foam.

An order of thin edges at a vertex can be reversed by adding three dots, one on each adjacent edge, as shown in relation (1) in Figure 15, with an additional dot added on both sides of the relation on the $(a+b)$-line. Two dots on the $(a+b)$-line on the left hand side can then be cancelled via the Figure 41 cobordism. Dots can be split off as well and removed, being null-cobordant (Figure 46).

A combination of these moves transforms U_0 into a cobordant foam which is a disjoint union of foams U_{a_i,b_i} and a braid-like foam U_2 without crossings, dots, and compatible orders of thin edges at all vertices, see Figure 17 on the right. Foam U_2 is null-cobordant, as explained earlier. Foam $U_{a,b}$ is null-cobordant as well, as shown in Figure 47. Consequently, U is null-cobordant.

4.2 Foams with a map into a topological space

Consider 1-foams and 2-foams equipped with a continuous map into a topological space X. Without loss of generality we can assume that X is a connected CW-complex. One can form the abelian group $\mathrm{Cob}^{1,X}_{\mathbb{R}_{>0}}$ of $\mathbb{R}_{>0}$-decorated oriented 1-foams U with a map $\psi : U \longrightarrow X$

modulo cobordisms. Two 1-foams as above with maps $\psi_i : U_i \longrightarrow X$ are cobordant if there is a 2-foam F with a continuous map $\psi : F \longrightarrow X$ such that $\partial(F,\psi) = (U_1,\psi_1) \sqcup (-U_0,\psi_0)$. For the sake of simplicity, we can further assume that X is a path-connected CW-complex.

The homotopy classes of maps $\psi : U \longrightarrow X$ of a 1-foam into X depend only on the fundamental group $\pi_1(X)$ of X. Denote this group by G and consider G-decorated 1-foams, as follows. A decoration consists of finitely many dots on edges of U, each dot labeled by an element of G. Form the standard model of the classifying space BG, take its 2-skeleton and pass to the Poincaré dual $P(G)$ of the 2-skeleton. A map of a 1-foam to BG can be deformed to a piecewise linear (PL) map into the 1-skeleton BG^1 of BG, which we also denote $\psi : U \longrightarrow \mathsf{BG}^1$. Here we view the 1-skeleton of BG as a subspace of $P(G)$. The inverse image of the 1-skeleton of $P(G)$ is then a collection of points on the edges of U labeled by elements of G. A point labeled $g \in G$ corresponds to the intersections of $\psi(U)$ with the one-cell of $P(G)$ labeled g. Also see [9, Section 2].

A cobordism F between 1-foams U_1, U_2 which is a 2-foam with a map $\psi : F \longrightarrow X$ can be converted to a PL map into the 2-skeleton $P(G)$, also denoted ψ. The inverse image of the 1-skeleton $P(G)^1$ of $P(G)$ is then a one-dimensional PL CW-complex in F with labels on edges, with possible singularities as shown in Figure 48. The edges labeled $1 \in G$ can be erased.

Proposition 4.3. The cobordism group of oriented $\mathbb{R}_{>0}$-decorated 1-foams equipped with a continuous map to a path-connected CW-complex X is given by

$$(\mathbb{R} \otimes_{\mathbb{Z}} \mathrm{H}_1(X,\mathbb{Z})) \oplus (\mathbb{R} \wedge_{\mathbb{Q}} \mathbb{R}). \tag{48}$$

Note that, if $\mathrm{H}_1(X,\mathbb{Z})$ is torsion, the first term vanishes.

Proof. Denote by $[g]$ the image of $g \in G$ in $\mathrm{H}_1(G) = \mathrm{H}_1(X,\mathbb{Z})$ and define a map

$$\gamma_1 \ : \ \mathsf{Cob}^{1,X}_{\mathbb{R}_{>0}} \longrightarrow \mathbb{R} \otimes_{\mathbb{Z}} \mathrm{H}_1(X,\mathbb{Z}) \tag{49}$$

by sending a G-labeled oriented 1-foam U to the sum

$$\gamma_1(U) \ := \ \sum_i a_i \otimes [g_i], \tag{50}$$

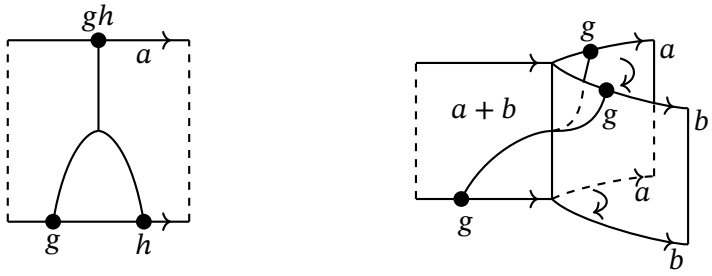

Figure 48: Possible singularities of a network of G-defects on a 2-foam. Trivalent vertices of the network on a facet (left figure) are points in $\psi^{-1}(P(G)^0)$, where $P(G)^0$ is the 0-skeleton of the Poincaré dual $P(G)$. Unlike that in Figure 44 on the right, the order of thin facets does not reverse when a defect line crosses a seam (right figure).

where the sum is over all labels $g_i \in G$ on U and a_i is the thickness of the edge which contains g_i. It is clear that γ_1 is invariant under cobordisms between 1-foams shown in Figure 48. Topology changes of 1-foams under cobordisms, shown in Figure 16, happen away from the one-dimensional network of G-defects on a cobordism, since the latter network can be deformed away from vertices and from local maxima and minima of seams and facets. Consequently, $\gamma_1(U)$ depends only on the cobordism class of U in $\mathsf{Cob}^{1,X}_{\mathbb{R}_{>0}}$, so it is a well-defined map on cobordism classes $[U]$. Define the homomorphism

$$\gamma \;:\; \mathsf{Cob}^{1,X}_{\mathbb{R}_{>0}} \longrightarrow (\mathbb{R} \otimes_{\mathbb{Z}} \mathrm{H}_1(X,\mathbb{Z})) \oplus (\mathbb{R} \wedge_{\mathbb{Q}} \mathbb{R}), \;\; \gamma([U]) = (\gamma_1([U]), \mathsf{SAF}(U)). \tag{51}$$

It is then straightforward to check that γ is an isomorphism of groups. Indeed, the defect points on a 1-foam U can be split away, each on its own circle, from the rest of U, converting U into the disjoint union of a foam U' without G-defects and a union U'' of circles $C_1, \ldots, C_n$ carrying labels $g_1, \ldots, g_n$ and having thicknesses $a_1, \ldots, a_n$. The cobordism class of U' is an element of $\mathbb{R} \wedge_{\mathbb{Q}} \mathbb{R}$, and that of U'' reduces to an element of $\mathbb{R} \otimes_{\mathbb{Z}} \mathrm{H}_1(X,\mathbb{Z})$ as outlined above. The homomorphism γ in (51) has a section s taking a generator $a \otimes g$ in the first term on the RHS to a circle of thickness a carrying label g, and a generator $a \wedge b$ of the second term on the RHS to the web $U_{a,b}$ shown in Figure 14, see the discussion in that section. We have $\gamma \circ s = 1$. Our classification of the cobordism group without

G-decorations in Theorem 2.6 and the above arguments, including splitting off G-points away from the rest of the 1-foam, imply that $s \circ \gamma = 1$, showing that γ is an isomorphism and concluding the proof. □

4.3 Other variations

Remark 4.4. D. Sullivan in [33, 35] has proved that any oriented one-dimensional solenoidal manifold M is the boundary of an oriented solenoidal surface. The idea (tributing his much earlier conversation with B. Edwards) is to represent M as the closure of a braid-like structure, that is, as the mapping torus of a homeomorphism of the Cantor set. Sullivan then uses R. D. Anderson's theorem [2] that the homeomorphism group of the Cantor set is simple and, in particular, perfect. Representing the homeomorphism as a product of commutators allows to realize M as the boundary, schematically shown in Figure 12. This use of braid-like closures is analogous to that in the proofs of Theorems 2.6, 4.1, where an oriented weighted 1-foam is represented as the closure of a braid 1-foam. It is likely that Sullivan's result can be interpreted as the vanishing of K_1 of a suitable assembler category [37, 38], where the assembler structure is that of coverings of the Cantor set.

Remark 4.5. The SAF invariant can be generalized to the Kenyon–Smillie invariant [15, 6], and it is an interesting question to interpret the latter via suitably decorated foam cobordisms.

Remark 4.6. O. Lacourte [19] defines a version of interval exchange transformations for each subgroup $\Gamma \subset \mathbb{R}/\mathbb{Z}$, via the corresponding subgroup $\mathsf{IET}(\Gamma)$ of the group $\mathsf{Aut}_{\mathsf{IET}}$. He establishes an isomorphism between $H_1(\mathsf{IET}(\Gamma))$ and the second skew-symmetric power of $\widetilde{\Gamma}$ over $\mathbb{Z}$, where $\widetilde{\Gamma}$ is the preimage of Γ in $\mathbb{R}$. It is straightforward to extend the results of Section 2 to interpret the above first homology group as the group of foam cobordisms, with the facets of foams carrying weights in $\widetilde{\Gamma} \cap \mathbb{R}_{>0}$ (and see Remark 2.9).

Lacorte also considers the group of IETs with flips. This group is known to be perfect, and Theorem 4.1 is a foam interpretation of this result. Lacourte shows that subgroups

$\mathrm{IET}(\Gamma)$ with flips modulo the commutator may have 2-torsion, and there should be an analogue of this result for foam cobordism.

Acknowledgments

The authors are grateful to David Gepner, Nitu Kitchloo, and Inna Zakharevich for interesting discussions. The authors would like to thank the referees for detailed feedback on our paper. M.K. would like to acknowledge partial support from NSF grant DMS-2204033 and Simons Collaboration Award 994328.

References

[1] J. F. Adams. *Stable homotopy and generalised homology*. Chicago Lectures in Mathematics. University of Chicago Press, Chicago, Ill.-London, 1974. 46

[2] Richard D. Anderson. The algebraic simplicity of certain groups of homeomorphisms. *Amer. J. Math.*, 80:955–963, 1958. 54

[3] Pierre Arnoux. Échanges d'intervalles et flots sur les surfaces. In *Ergodic theory (Sem., Les Plans-sur-Bex, 1980) (French)*, volume 29 of *Monogr. Enseign. Math.*, pages 5–38. Univ. Genève, Geneva, 1981. 48

[4] Pierre Arnoux. *Un invariant pour les echanges d'intervalles et les flots sur les surfaces*. HAL theses, 1981. Thesis (Ph.D.)–Université de Reims Champagne-Ardenne. 48

[5] Skew of 2-cocycle for trivial group action of abelian group is alternating bihomomorphism. https://groupprops.subwiki.org/wiki/Skew_of_2-cocycle_for_trivial_group_action_of_abelian_group_is_alternating_bihomomorphism, 2012. 32

[6] Kariane Calta. Veech surfaces and complete periodicity in genus two. *J. Amer. Math. Soc.*, 17(4):871–908, 2004. 54

[7] Carmen Caprau, Gabriel Coloma, and Marguerite Davis. The L-move and Markov theorems for trivalent braids. *Involve*, 13(1):21–50, 2020. 21

[8] Hieu Trung Do and Thomas A. Schmidt. New infinite families of pseudo-Anosov maps with vanishing Sah-Arnoux-Fathi invariant. *J. Mod. Dyn.*, 10:541–561, 2016. 3

[9] David Gepner, Mee Seong Im, Mikhail Khovanov, and Nitu Kitchloo. Foams with flat connections and algebraic K-theory. *arXiv preprint arXiv:2405.14465*, pages 1–57, 2024. 2, 21, 52

[10] Yonatan Harpaz. Complex Cobordism and Formal Group Laws. *Online lecture notes, https://www.math.univ-paris13.fr/ harpaz/complex_cobordism.pdf*, pages 1–19, 2012. 46

[11] Mee Seong Im and Mikhail Khovanov. Entropy, cocycles, and their diagrammatics. *arXiv preprint arXiv:2409.08462*, pages 1–82, 2024. 29

[12] Atsushi Ishii. The Markov theorems for spatial graphs and handlebody-knots with Y-orientations. *Internat. J. Math.*, 26(14):1550116, 23, 2015. 21

[13] Ken Kanno and Kouki Taniyama. Braid presentation of spatial graphs. *Tokyo J. Math.*, 33(2):509–522, 2010. 21

[14] Louis H. Kauffman. Invariants of graphs in three-space. *Trans. Amer. Math. Soc.*, 311(2):697–710, 1989. 16

[15] Richard Kenyon and John Smillie. Billiards on rational-angled triangles. *Comment. Math. Helv.*, 75(1):65–108, 2000. 54

[16] Mikhail Khovanov. $\mathfrak{sl}(3)$ link homology. *Algebr. Geom. Topol.*, 4:1045–1081, 2004. 2

[17] Mikhail Khovanov and Nitu Kitchloo. A deformation of Robert-Wagner foam evaluation and link homology. In *Algebraic and topological aspects of representation theory*, volume 791 of *Contemp. Math.*, pages 147–204. Amer. Math. Soc., Providence, RI, 2024. 2

[18] Peter B. Kronheimer and Tomasz S. Mrowka. Tait colorings, and an instanton homology for webs and foams. *J. Eur. Math. Soc. (JEMS)*, 21(1):55–119, 2019. 2

[19] Octave Lacourte. Abelianization of some groups of interval exchanges. *Ann. Inst. Fourier (Grenoble)*, 72(1):59–108, 2022. 48, 54

[20] Marco Mackaay and Pedro Vaz. The universal $\mathfrak{sl}_3$-link homology. *Algebr. Geom. Topol.*, 7:1135–1169, 2007. 2

[21] J. Peter May. *A concise course in algebraic topology*. Chicago Lectures in Mathematics. University of Chicago Press, Chicago, IL, 1999. 46

[22] James R. Munkres. *Topology*. Prentice Hall, Inc., Upper Saddle River, NJ, second edition, 2000. 22

[23] Ulrich Oertel. Incompressible branched surfaces. *Invent. Math.*, 76(3):385–410, 1984. 9

[24] Ulrich Oertel. Measured laminations in 3-manifolds. *Trans. Amer. Math. Soc.*, 305(2):531–573, 1988. 6, 9

[25] Robert C. Penner and John L. Harer. *Combinatorics of train tracks*, volume 125 of *Annals of Mathematics Studies*. Princeton University Press, Princeton, NJ, 1992. 24, 25

[26] Eric Peterson. *Formal geometry and bordism operations*, volume 177 of *Cambridge Studies in Advanced Mathematics*. Cambridge University Press, Cambridge, 2019. With a foreword by Matthew Ando. 46

[27] Hoel Queffelec and Kevin Walker. Movie moves for framed foams from multijet transversality. *arXiv preprint arXiv:2205.14947*, pages 1–88, 2022. 6, 7

[28] Louis-Hadrien Robert and Emmanuel Wagner. A closed formula for the evaluation of foams. *Quantum Topol.*, 11(3):411–487, 2020. 2

[29] Louis-Hadrien Robert and Emmanuel Wagner. Symmetric Khovanov-Rozansky link homologies. *J. Éc. polytech. Math.*, 7:573–651, 2020. 7

[30] David E. V. Rose and Paul Wedrich. Deformations of colored $\mathfrak{sl}_N$ link homologies via foams. *Geom. Topol.*, 20(6):3431–3517, 2016. 2

[31] Markus Spitzweck. Algebraic cobordism in mixed characteristic. *Homology Homotopy Appl.*, 22(2):91–103, 2020. 46

[32] Neil P. Strickland. Formal groups. https://strickland1.org/courses/formalgroups/fg.pdf, pages 1–63, 2019. 46

[33] Dennis Sullivan. Solenoidal manifolds. *J. Singul.*, 9:203–205, 2014. 54

[34] William A. Veech. The metric theory of interval exchange transformations. III. The Sah-Arnoux-Fathi invariant. *Amer. J. Math.*, 106(6):1389–1422, 1984. 3

[35] Alberto Verjovsky. Commentaries on the paper “Solenoidal Manifolds" by Dennis Sullivan. *J. Singul.*, 9:245–251, 2014. 54

[36] Yaroslav Vorobets. Notes on the commutator group of the group of interval exchange transformations. *arXiv preprint arXiv:1109.1352*, pages 1–16, 2011. 3, 11

[37] Inna Zakharevich. The K-theory of assemblers. *Adv. Math.*, 304:1176–1218, 2017. 3, 21, 54

[38] Inna Zakharevich. On K_1 of an assembler. *J. Pure Appl. Algebra*, 221(7):1867–1898, 2017. 3, 11, 14, 21, 54

[39] Anton Zorich. Flat surfaces. In *Frontiers in number theory, physics, and geometry. I*, pages 437–583. Springer, Berlin, 2006. 25

[40] Anton Zorich. Geodesics on flat surfaces. In *International Congress of Mathematicians. Vol. III*, pages 121–146. Eur. Math. Soc., Zürich, 2006. 25

Foam cobordism and the Sah-Arnoux-Fathi invariant

AUTHORS

Mee Seong Im
Department of Mathematics
Johns Hopkins University
Baltimore, MD 21218, USA
and
Department of Mathematics
United States Naval Academy
Annapolis, MD 21402, USA
email: meeseong@jhu.edu

Mikhail Khovanov
Department of Mathematics
Johns Hopkins University
Baltimore, MD 21218, USA
and
Department of Mathematics
Columbia University
New York, NY 10027, USA
email: khovanov@jhu.edu